Journal of Mammalian Evolution (2022) 29:1–26
https://doi.org/10.1007/s10914-021-09564-7

ORIGINAL PAPER

A New Mammal Skull from the Late Cretaceous of Romania and Phylogenetic Affinities of Kogaionid Multituberculates

Thierry Smith[1] · Vlad A. Codrea[2,3] · Ghéreint Devillet[1] · Alexandru A. Solomon[2,3]

Accepted: 7 July 2021 / Published online: 24 September 2021

Abstract

Among the Late Cretaceous fossil sites of Europe, only those from the so-called "Haţeg Island" in Transylvania, western Romania, are remarkable by their abundance in mammal remains. Curiously, all of them belong to a single family of multituberculates, the Kogaionidae, one of the rare families that survived the Cretaceous-Paleogene mass extinction in Europe. Kogaionids are mostly represented by isolated teeth except for three partial large skulls from the Maastrichtian Sânpetru Formation of the Haţeg Basin that have been described from the Sânpetru locality as *Kogaionon ungureanui* and from the Pui locality as *Barbatodon transylvanicus* and *Litovoi tholocephalos*. Here we report for the first time the discovery of a partial skull associated with p4 of a small-sized kogaionid from the Nălaţ-Vad locality in the Sânpetru Formation that we refer to *Kogaionon radulescui*, sp. nov. An updated phylogenetic analysis, including seven Maastrichtian and Paleocene kogaionids is performed and confirms that Kogaionidae is a monophyletic clade at the base of Cimolodonta. *Kogaionon* differs from *Barbatodon* in its narrower snout, proportionally smaller P1, narrower anterior part of P4 with four similar-sized cusps in the middle row, more squared or rounded M1 with an anteroposteriorly longer lingual row, and shorter p4 (at least for *K. radulescui*). *Litovoi tholocephalos* is here considered to be a junior synonym of *B. transylvanicus*. Despite their Maastrichtian age, the very simple and conservative dental morphology of these Romanian kogaionids suggests that they originated from an eobaatarid-like ancestor dispersing from Asia or possibly already existing in Europe between the Barremian and Albian, 40 to 55 Ma earlier.

Keywords Mammalia · Multituberculata · Maastrichtian · Haţeg Basin · Romania

Introduction

Over the last 25 years, knowledge of the anatomy and diversity of multituberculate mammals has made significant progress thanks to numerous discoveries and important studies (e.g., Kielan-Jaworowska and Gambaryan 1994; Kielan-Jaworowska and Hurum 1997, 2001; Hurum 1998; Wible and Rougier 2000; Kielan-Jaworowska and Lancaster 2004; Kusuhashi et al. 2009, 2010, 2020; Wilson et al. 2012; Yuan et al. 2013; Codrea et al. 2014; Smith and Codrea 2015; Xu et al. 2015; Rougier et al. 2016; Solomon et al. 2016; Csiki-Sava et al. 2018; Wang et al. 2019; Wible et al. 2019; Mao et al. 2020; Weaver et al. 2020). However, the systematics, phylogeny, and origin of multituberculates are still not well understood (Kielan-Jaworowska and Hurum 2001; Averianov et al. 2020, and references therein). This is especially true for European Cretaceous multituberculates for which phylogenetic relationships with other groups are difficult to establish.

Among the Late Cretaceous mammal sites of Europe, only those from Transylvania in western Romania, are remarkable in their abundance of multituberculate remains (Grigorescu et al. 1999; Codrea et al. 2002). Multituberculate specimens were discovered in the Sânpetru Formation of the Haţeg Basin, which allowed description of *Kogaionon ungureanui* from the Sânpetru locality (Rădulescu and

✉ Thierry Smith
thierry.smith@naturalsciences.be

[1] Directorate Earth & History of Life, Royal Belgian Institute of Natural Sciences, Rue Vautier 29, B-1000 Brussels, Belgium

[2] Faculty of Biology and Geology, Laboratory of Paleotheriology and Quaternary Geology, University Babeş-Bolyai, 1 Kogălniceanu Str, 400084 Cluj-Napoca, Romania

[3] Department of Natural Sciences, Mureș County Museum, 24 Horea Str, 540036 Târgu Mureș, Romania

Samson 1996, 1997) and *Barbatodon transylvanicus* and its very similar sister taxon *Litovoi tholocephalos*, both from the Pui locality (Rădulescu and Samson 1986; Grigorescu and Hahn 1987; Csiki-Sava et al. 2018). Northeast of the Haţeg Basin (Fig. 1), the Transylvanian Basin revealed the existence of a very small kogaionid, *Barbatodon oardaensis*, at the Oarda de Jos locality in the Şard Formation (Codrea et al. 2014). *Barbatodon oardaensis* was also found in an unnamed formation of the Negoiu locality in the Rusca Montană Basin, located west of the Haţeg Basin (Codrea et al. 2017a).

In addition to remains of these formally described species, numerous specimens left in open nomenclature were also found in the Şard Formation (= Sebeş Formation in Csiki-Sava et al. 2016; see Codrea and Dica 2005; Codrea et al. 2010 and Solomon et al. 2020 for details) of Petreşti locality in the Transylvanian Basin (Vremir et al. 2014) and the Densuş-Ciula Formation of Tuştea and Vălioara localities, and the Sânpetru Formation of Toteşti and Nălaţ-Vad localities, in the Haţeg Basin (Csiki and Grigorescu 2000; Codrea et al. 2002, 2017a; Smith et al. 2002). Unfortunately, most of the material is composed of isolated teeth. In opposition to placental posterior cheek teeth, multituberculate isolated teeth are difficult to associate because of their great morphological differences from one dental position to another, even within the same tooth row. Until now, only three species have been described based on specimens bearing associated teeth: *K. ungureanui* known by a briefly described partial skull from Sânpetru (Rădulescu and Samson 1996, 1997) and *B. transylvanicus* and *L. tholocephalos* known by partial skulls, associated dentaries, and postcranial remains from Pui (Csiki et al. 2005; Smith and Codrea 2015; Solomon et al. 2016; Csiki-Sava et al. 2018). The three taxa represent mid- to large-sized kogaionid multituberculates.

Here we describe a partial skull associated with p4 of a new, small-sized multituberculate from Nălaţ-Vad (Fig. 2). We also describe from the same locality a dentary fragment with i1 and p4 that we refer to the same species as the skull based on the similar morphology of both p4s. The locality was discovered in the early days of June 2001 by one of us (VAC) and Cristina Fărcaș at the end of the second Romanian-Belgian excavation campaign in Transylvania, which was composed of the University Babeş-Bolyai of Cluj-Napoca and the Royal Belgian Institute of Natural Sciences (see Smith et al. 2002 for the first description of the site). The fossil layers are of fluviatile origin and belong to the lower Maastrichtian Sânpetru Formation, which is exposed in the bed of the Râul Mare river, between the villages of Nălaţ and Vad (Fig. 1). The locality has yielded remains of albanerpetontid amphibians, lacertilians, crocodilians, and kogaionid mammals (Smith et al. 2002), the stem Testudines turtle *Kallokibotion bajazidi* (Peréz-García and Codrea 2018; Martín-Jiménez et al. 2021), the iguanodontian *Zalmoxes shqiperorum* (Godefroit et al. 2009), the titanosaur *Paludititan nalatzensis* (Csiki et al. 2010), a *Martinavis*-like euenantiornith bird (Wang et al. 2011), and, more recently, a *Gargantuavis*-like theropod (Mayr et al. 2020). The

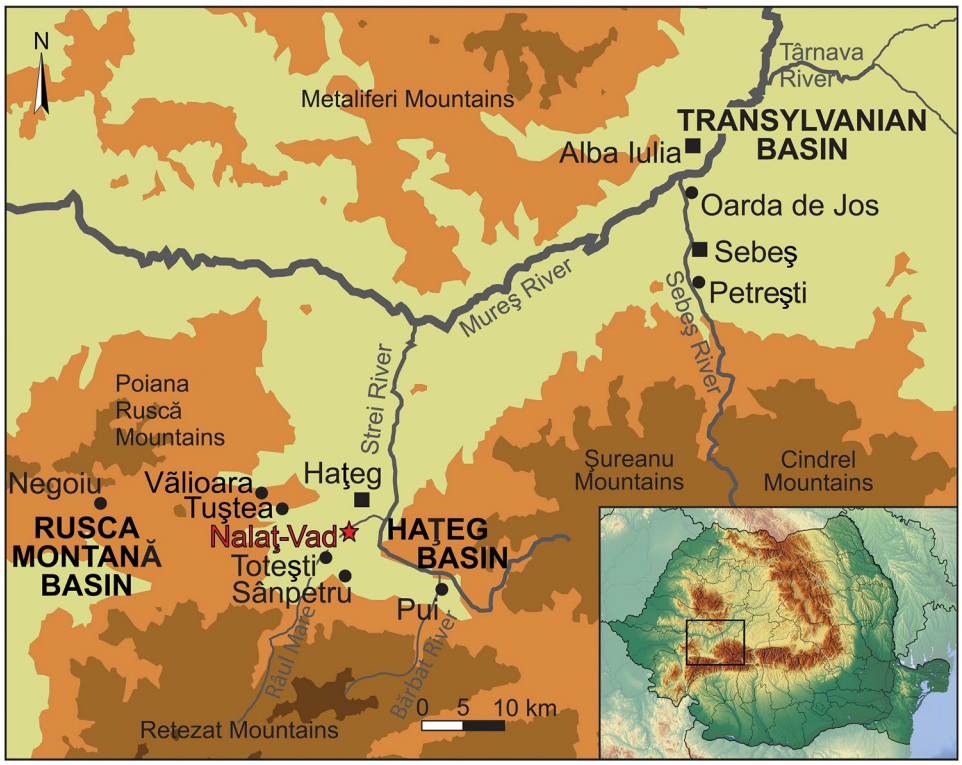

Fig. 1 Location of the main Maastrichtian continental localities of the Transylvanian, Haţeg, and Rusca Montană basins (Romania) that have yielded kogaionid multituberculate mammal remains (black dots). The specimens PSMUBB V-893 and UBB NV-Mt1 of *Kogaionon radulescui* sp. nov. were discovered in the locality of Nălaţ-Vad (red star)

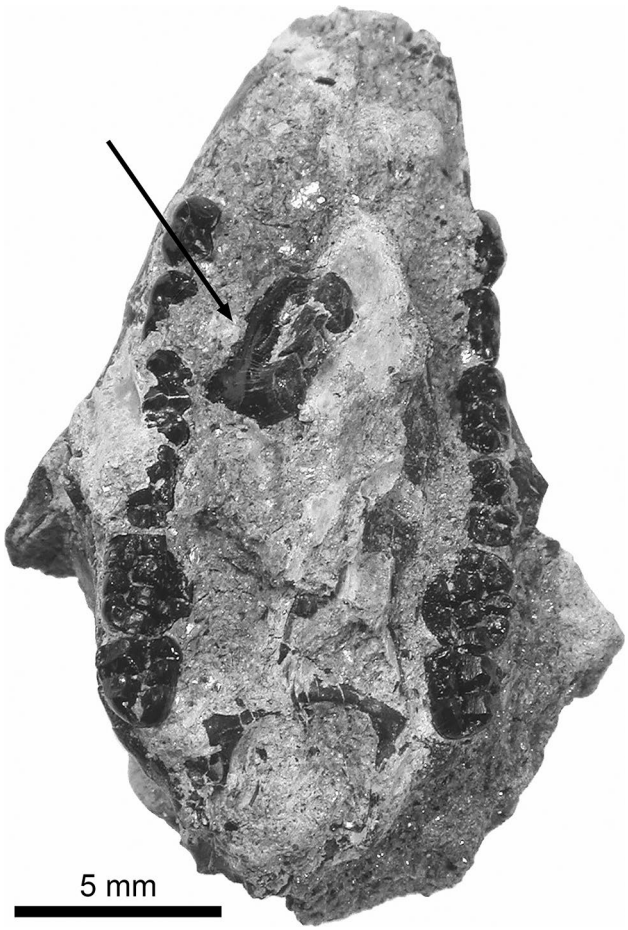

Fig. 2 Partial cranium PSMUBB V-893 of *Kogaionon radulescui*, sp. nov., in its original grey marl matrix showing upper teeth and left p4 (arrow) associated together before preparation

composition of the Nălaţ-Vad fauna, like the other Maastrichtian vertebrate faunas of Transylvania, is typical of the supposedly insular environment that prevailed in the Late Cretaceous European archipelago (e.g., Csiki-Sava et al. 2015). The small mammal skull from Nălaţ-Vad belongs to the Kogaionidae, the only multituberculate family known from Romania so far. Due to the difficult identification of tooth positions, this family has been regarded as aberrant while being tentatively assigned to the most primitive cimolodontans, the *Paracimexomys* group, pending further discoveries (Kielan-Jaworowska and Hurum 2001; Kielan-Jaworowska et al. 2004).

Material and Methods

Institutional Abbreviations

ISB, Institute of Speleology "Emil Racoviţă," Bucharest, Romania; **IVPP,** Institute of Vertebrate Paleontology and Paleoanthropology, Chinese Academy of Sciences, Beijing, China; **LPB (FGGUB),** Laboratory of Paleontology, Faculty of Geology and Geophysics, University of Bucharest, Romania; **MOR,** Museum of the Rockies, Bozeman, Montana; **PSMUBB,** Palaeontology-Stratigraphy Museum, University Babeş-Bolyai, Cluj-Napoca, Romania; **RBINS** (IRSNB)**,** Royal Belgian Institute of Natural Sciences, Brussels, Belgium; **UBB ODAN-Mt, UBB P-Mt, UBB NV-Mt,** Laboratory of Paleotheriology and Quaternary Geology collection (Oarda de Jos, Pui and Nălaţ-Vad Multituberculata), University Babeş-Bolyai, Cluj-Napoca, Romania; **UCM FNT,** Department of Paleontology (Fontllonga mammal collection), Universidad Complutense de Madrid, Spain.

Material Collected

The partial cranium associated with p4 was originally embedded in a grey marl matrix discovered by one of us (VAC) at Nălaţ-Vad in May 2004 (Fig. 2). The dentary fragment with i1 and p4 was discovered at Nălaţ-Vad in May 2002 during the Romanian -Belgian excavation campaigns in Transylvania. The preparation of both specimens was done with tungsten carbide needles at the RBINS. The cranium is deposited in the Museum of Paleontology-Stratigraphy under the number PSMUBB V-893 and the dentary fragment in the Laboratory of Paleotheriology and Quaternary Geology under the number UBB NV-Mt1, both at the University Babeş-Bolyai of Cluj-Napoca, Romania.

Photography

The specimens are black and were therefore covered with ammonium chloride for photography. Close-ups of the teeth of PSMUBB V-893 were taken with a low environmental scanning electronic microscope (ESEM Quanta 200).

Terminology

Anatomical terminology used for bones as well as tooth position follows Kielan-Jaworowska et al. (2004). Therefore, cusp formulae on premolars and molars are based on the number of cusps in consecutive rows and given from labial to lingual separated by a colon. Measurements were taken using digital calipers to two decimal places.

Cladistic Analysis

A cladistic analysis was performed based on the most recent character matrices for multituberculates (Csiki-Sava et al. 2018; Wang et al. 2019; Weaver et al. 2020). The phylogenies of Weaver et al. (2020) and Wang et al. (2019) are quite close to each other. The one of Weaver et al. (2020) was used in the description of the new basal ptilodontoid *Filikomys*, the composite taxon *Cimexomys*, present until then in the

previous matrices having been removed because "the majority of its character scores were based on MOR 302, a specimen that is now assigned to *Filikomys primaevus*" (Weaver et al. 2020: Suppl. p. 25). The phylogeny of Wang et al. (2019) is similar to that of Csiki-Sava et al. (2018) except that it includes five added taxa and 23 added characters for assessing the phylogenetic relationships of the eobaatarid plagiaulacidan *Jeholbaatar kielanae*. The matrix of Csiki-Sava et al. (2018) focused on the kogaionid cimolodontan *Litovoi tholocephalos* and was based on those of Xu et al. (2015) and Mao et al. (2016), which were based on the phylogeny of Yuan et al. (2013). The last is also notably based on the classic phylogenies of Kielan-Jaworowska and Hurum (2001) and Rougier et al. (1997). The present modified matrix (Supplementary Appendix S2) is also partly based on the one of Kusuhashi et al. (2020), which included some scores for previously unknown characters of the eobaatarid genera *Sinobaatar*, *Heishanobaatar*, and *Hakusanobaatar*. Similarly, we scored numerous previously unknown characters of *Pentacosmodon* based on the monograph of Fox (2005) on western Canadian microcosmodontids. However, we first checked and corrected numerous character scores in the resulting matrix (see details in Phylogenetic analysis). The scoring was then expanded based on our firsthand study of the new kogaionid cranium and dentary fragment, as well as other kogaionid species, including *Barbatodon oardaensis* and two *Hainina* species: *H. belgica* and *H. pyrenaica* (Vianey-Liaud 1979; Peláez-Campomanes et al. 2000). Since the problematic *Paracimexomys* group (e.g., *Cimexomys*), the most plesiomorphic informal group of Cimolodonta (for a discussion see Eaton and Cifelli 2001: 467–469; Kielan-Jaworowska et al. 2004: 320–321), has disappeared from the most recent analyses, we included *Bryceomys* in our analysis. We scored *Bryceomys* based on the works of Eaton (1995) and Eaton and Cifelli (2001) because this genus is clearly defined and older (Albian-Cenomanian through Turonian) than the debatable composite genera *Paracimexomys* and *Cimexomys*, which are both represented by numerous species of different ages extended from the Early Cretaceous (Aptian–Albian) to the early Paleocene.

The final resulting matrix (55 taxa scored for 130 characters) was analyzed as described by Weaver et al. (2020), using the heuristic searches of PAUP* (version 4.0a169, Swofford 2003), random addition sequence, 100,000 replications, one tree held at each step, tree-bisection-reconnection (TBR) branch-swapping algorithm with reconnection limit of eight, steepest descent option not in effect, initial 'Maxtrees' setting of 100,000, and 'MulTrees' option not in effect. The only difference with Weaver et al. (2020) is that we did not consider 19 characters ordered (characters 17, 25, 26, 29, 31, 32, 43, 46, 47, 48, 49, 51, 52, 55, 58, 59, 61, 72, 85) but only 17. Characters 48 and 55 were considered as unordered (see Phylogenetic analysis).

All data generated or analyzed during this study are included in this published article [and its supplementary information files].

Systematic Paleontology

Class Mammalia Linnaeus, 1758
Subclass Allotheria Marsh, 1880
Order Multituberculata Cope, 1884
Suborder Cimolodonta McKenna, 1975
Family Kogaionidae Rădulescu and Samson, 1996
Genus *Kogaionon* Rădulescu and Samson, 1996

Type species *Kogaionon ungureanui* Rădulescu and Samson, 1996

Emended diagnosis Small- to large-sized kogaionid genus differing from *Barbatodon* in its narrower snout, proportionally smaller P1, smaller ratio of P1-4/M1-2, P4 narrower anteriorly and with four cusps of similar size and aspect in the middle row, longer lingual row of M1, and shorter p4; differing from *Hainina* in possessing P3 with three cusps in the lingual row (instead of five), P4 with four individualized cusps in the middle row (absence of crest), shorter lingual row of M1 with only 2–3 cusps, and wider posterior part of p4.

Kogaionon radulescui, sp. nov.
(Figs. 2–7 and Tables 1, 2).

Holotype PSMUBB V-893, partial cranium (V-893a) and associated left p4 (V-893b).

Referred specimen UBB NV-Mt1, a left dentary fragment with i1 and p4.

Type locality Nălaţ-Vad, Râul Mare Valley, Haţeg Basin (Transylvania, Romania).

Type horizon Sânpetru Formation, Maastrichtian, Late Cretaceous.

Etymology Species dedicated to Constantin ('Costin') Rădulescu for his contribution to knowledge of kogaionid multituberculates.

Diagnosis Small-sized *Kogaionon* species about 35% smaller than *K. ungureanui*, 20% smaller than *Barbatodon transylvanicus* (= *Litovoi tholocephalos*), and 25% larger than *B. oardaensis*; further differs from *K. ungureanui* and *B. transylvanicus* by smaller ratio of P1-4/M1-2, and proportionally smaller P3; differs from *B. transylvanicus* in its longer lingual row of M1 and shorter p4; differs from *B. oardaensis* by the presence of only two cusps in the labial row of P3.

Table 1 Dental measurements (in mm) of *Kogaionon radulescui*, sp. nov., holotype PSMUBB V-893

Position	Right row		Left row	
	Length	Width	Length	Width
I3	1.18	0.89	-	-
P1	1.98	1.13	2.10	1.16
P2	2.20	1.25	2.06	1.25
P3	2.68	1.33	2.53	1.35
P4	2.18	1.35	2.24	1.31
M1	2.53	2.21	2.62	2.24
M2	2.22	2.13	2.18	2.14
p4	-	-	4.30	1.46

Table 2 Skull measurements (in mm) of *Kogaionon radulescui*, sp. nov., holotype PSMUBB V-893

Length of premaxilla (alveolar border)	~4.1
Length of premaxilla (nasal suture)	~6.4
Length of palate (contact premax.-maxillary suture and choanae)	14.9
Width of palate (between P4)	7.2
Depth of skull (above I2)	3.6
Depth of skull (above M2)	-
Maximum length of nasal	~14.2
Width of snout (contact premax.-maxillary suture and alveolar border in ventral view)	6.4
Width of snout (at the level of I2)	~4.7

Description

Cranium The fragmentary cranium PSMUBB V-893 is represented by a rostrum that preserves the nasals, the premaxillae (with the right I3), maxillae (broken posteriorly at the level of the anterior part of the zygomatic arches but preserving both complete upper cheek-tooth rows), palatines, and anterior fragments of the frontals (Fig. 3).

The rostrum is only slightly deformed at the level of the right premaxilla, which is slightly crushed and sunken in the ventral midline direction. Except for that part, the three-dimensional aspect of the rostrum is almost intact. The bones are preserved but fissured a little everywhere making the identification of sutures and foramina sometimes difficult. Some bones are damaged on the dorsal side, at the front of the snout, and the posterior margin of the rostrum; the lacrimal seems to not be preserved in dorsal view (Fig. 3a). The damage allows observation of a cast of what is possibly the left frontal sinus based on its lateral position and a partial cast of the left olfactory bulb (Fig. 3). The rostrum is as long as its base is wide at the level of infraorbital foramina.

Much of the nasal has flaked off the tip of the snout even the sediment is still present, showing relatively well its shape. The nasal is relatively long with about a little less than 50% of the anterior part in contact with the premaxilla. The posterior border of the nasal is about double the width

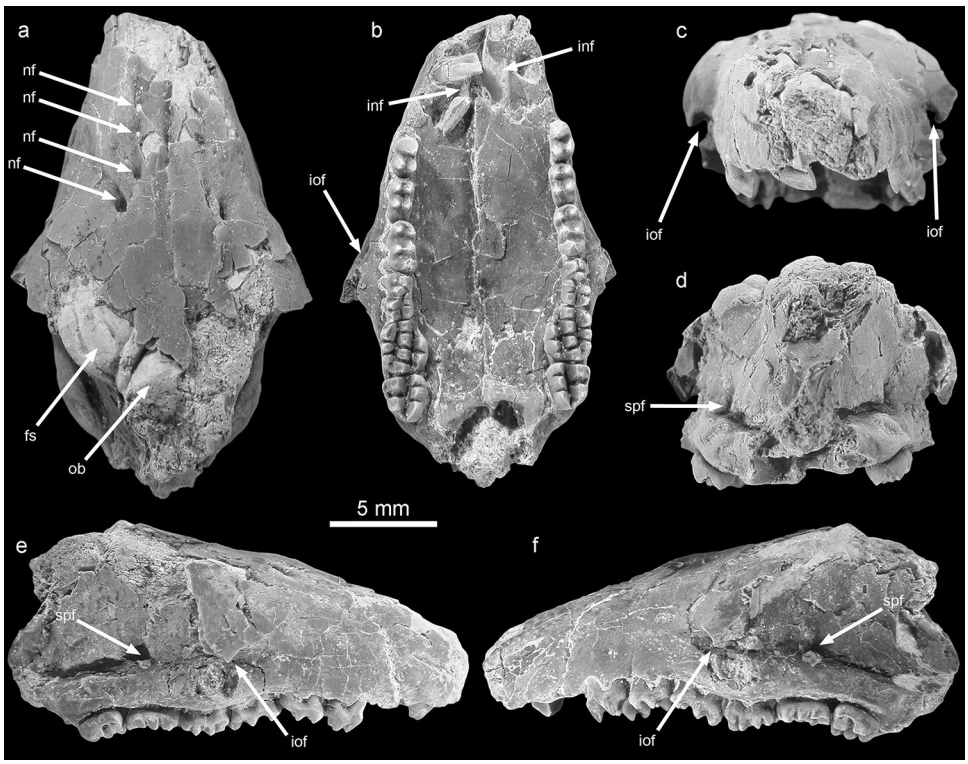

Fig. 3 Partial cranium PSMUBB V-893a of *Kogaionon radulescui*, sp. nov., in dorsal (**a**), ventral (**b**), anterior (**c**), posterior (**d**), right lateral (**e**), and left lateral (**f**) views. Abbreviations: fs, frontal sinus?; inf, incisive foramen; iof, infraorbital foramen; nf, nasal foramen; ob, olfactory bulb; spf, sphenopalatine foramen

of the anterior border. Four neurovascular foramina are visible on the left nasal, the two most posterior being the largest, especially the last one (Fig. 3a). Only the two large posterior neurovascular foramina are visible on the right nasal. The absence of the two smaller anterior foramina might be the result of a bilateral asymmetry or due to damage of that part of the bone.

Most of the frontals are not preserved and only two small fragments are present at the contact with the nasals on the midline of the skull roof. The suture between the nasals and the frontals seems pointed anteriorly and not deeply inserted between the nasals.

The premaxilla is well developed and of medium length in dorsal as well as ventral views by comparison with the short premaxillae of ptilodontoids and the long ones of djadochtatherioids. It is relatively narrow mediolaterally (Figs. 3a-b, 4a-b). The posterodorsal process is extended onto the roof of the rostrum (Figs. 3f, 4a-d). Ventrally, a large and anteroposteriorly elongate incisive foramen is visible within each premaxilla (Figs. 3b, 4b). Although the incisive foramen is posteriorly extended very near the border of the maxilla, it is difficult to establish if the maxilla contributes to its posterior border. The right incisive foramen is somewhat collapsed medio-laterally and is hidden on its posterior side by a fragment of bone. The left incisive foramen is broken on its medial side but its lateral side is preserved, showing that the anterior edge is at the level of the anterior border of the I3 alveolus. I3 is implanted marginally on the palatal part of the premaxilla and separated from the I2 alveolus by a short diastema. A slightly larger gap separates I3 from the posterior border of the premaxilla.

Both maxillae do not preserve the zygomatic arches and only their ventral and lateral sides provide information. The infraorbital foramen is oval with the long axis vertical and positioned at the level of the limit between P3 and P4 (Fig. 3b, c, e, f). Portions of the medial walls of the orbits are preserved, showing that the sphenopalatine foramina are located above M1s (Fig. 3d, e, f) and are prolonged posteriorly by deep sphenopalatine grooves on both sides of the skull (Fig. 3d). On the medial wall of the orbit, the maxillary-frontal suture seems visible, just above the sphenopalatine foramen and along the sphenopalatine groove. In ventral view, the anterior border of the maxilla is V-shaped and the root of the zygomatic process is at the level of the anterior root of P4 (Fig. 4b).

The palatine is relatively small, being about the same area as the M1 in ventral view (Fig. 4b). The contact of the palatine with the maxilla is at the level of the mid-length of M1. The shape of the palatine is approximatively square. No palatal vacuities are visible. The posterior border of the palatine has a well-developed postpalatine torus, which is ventrally projected, wide and moderately short anteroposteriorly (Fig. 4b). It forms a nearly tubular structure (Fig. 5b, d, e).

The sphenoid is partially preserved with the alisphenoid visible in ventral view at the contact of the palatine and the maxilla, just posteriorly to M2 (Fig. 4b). A fragment of the orbitosphenoid portion of the sphenoid seems preserved on the both sides of the skull (Fig. 4c, d). If correctly identified,

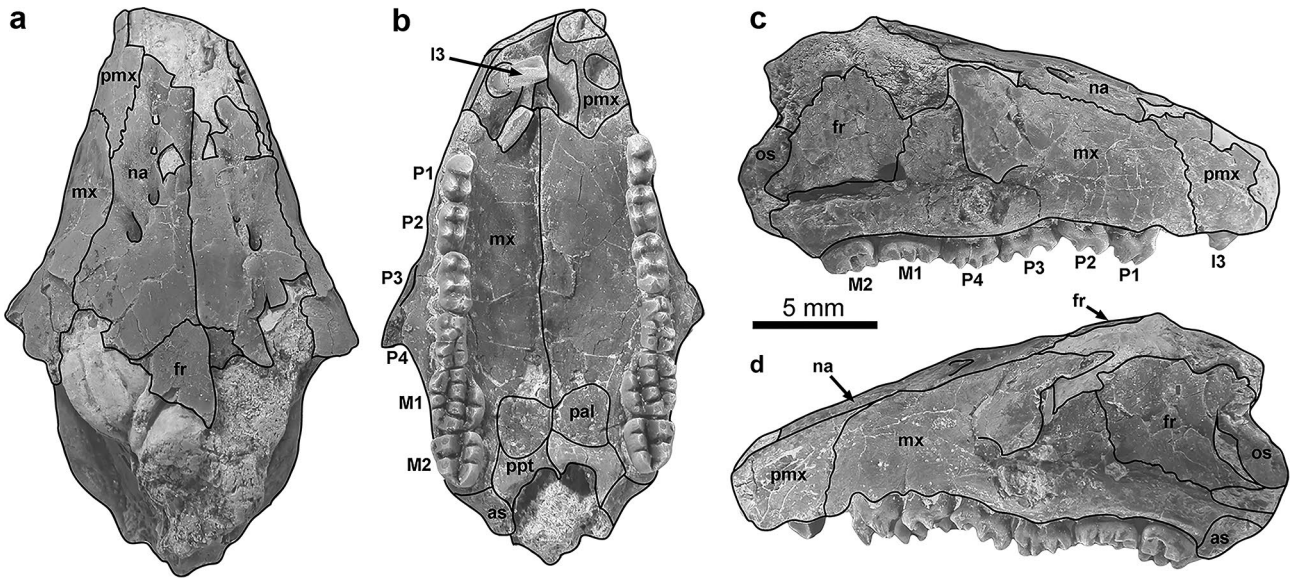

Fig. 4 Partial cranium PSMUBB V-893a of *Kogaionon radulescui*, sp. nov., with bone outlines in dorsal (**a**), ventral (**b**), right lateral (**c**), and left lateral (**d**) views. Abbreviations: as, alisphenoid; fr, frontal; mx, maxilla; na, nasal; os, orbitosphenoid; pal, palatine; pmx, premaxilla; ppt, postpalatine torus

it is detached on the left side, showing an opening that could delimitate the contact with the frontal anteriorly (Figs. 3f, 4d).

Dentary The dentary fragment represents only the anterior portion of the bone, being broken just posterior to p4 (Fig. 7). The diastema between i1 and p4 is estimated at 3.2 mm, taking into account the damage around the base of i1, which represents around 70% of the antero-posterior length of p4 (4.48 mm). The symphysis seems relatively short but this could possibly be exaggerated by the anterior part of the dentary bone, which is a bit damaged (Fig. 7a). In occlusal view, the angle formed by the surface of the symphysis and the lingual side of the horizontal ramus is around 35% (Fig. 7b). In labial view, the mental foramen is located below the diastema, very near i1 at the upper two-thirds of the height of the dentary (Fig. 7c).

Dentition The I2 is not preserved, but the left premaxilla preserves the I2 alveolus, which is damaged. Its diameter is about the same as that of I3 or slightly larger (Figs. 3b, 4b).

The I3 is preserved on the right premaxilla but it is sunken in the ventral midline direction and rotated somewhat counterclockwise (Figs. 3, 4, 6d-e). It is single-cusped, transversely wide, and anteroposteriorly compressed. The tip is worn, giving it a spatulate shape in anterior view. A very small bulge, slightly elongated, is present on the posterolabial side near the base of the tooth (Fig. 6d).

The P1 bears three cusps, the anterior one being the largest, almost as wide as the two posterior ones taken together (Figs. 3–5). The anterior cusp is a little lingually displaced and well distinct from the two posterior ones, which are closer to each other. There is a short flat surface forming a slope on the posterior part of the tooth, behind the cusps. That part represents about a quarter of the length of the tooth. In lateral view, it appears that the crown of P1 is higher than that of the other upper teeth (Fig. 3e, f). The crown and all the cusps of P1 look unworn. The enamel is relatively smooth with very weak wrinkles on the sides of lingual cusps. The most anterior cusp bears three thin crests that join at the tip (Fig. 5b, e). The posterolingual cusp bears four thin crests, the anterior one being the most marked. The posterolabial cusp does not bear discernible crests.

The P2 bears four cusps, the cusp formula being 2:2 (Figs. 3, 5). A small anterior cingulum joins the bases of the anterior labial and lingual cusps. All the cusps are similar in size and distinct from each other. The tooth also presents a flat posterior surface forming a gentle slope, similar to that on P1. That surface represents about a third of the length of the tooth. No wear is visible and weak wrinkles are present on the sides of the anterolingual cusp. Four thin crests joining at the tip are present on both lingual cusps (Fig. 5b, e). The anteroposterior crests are the most marked and connect

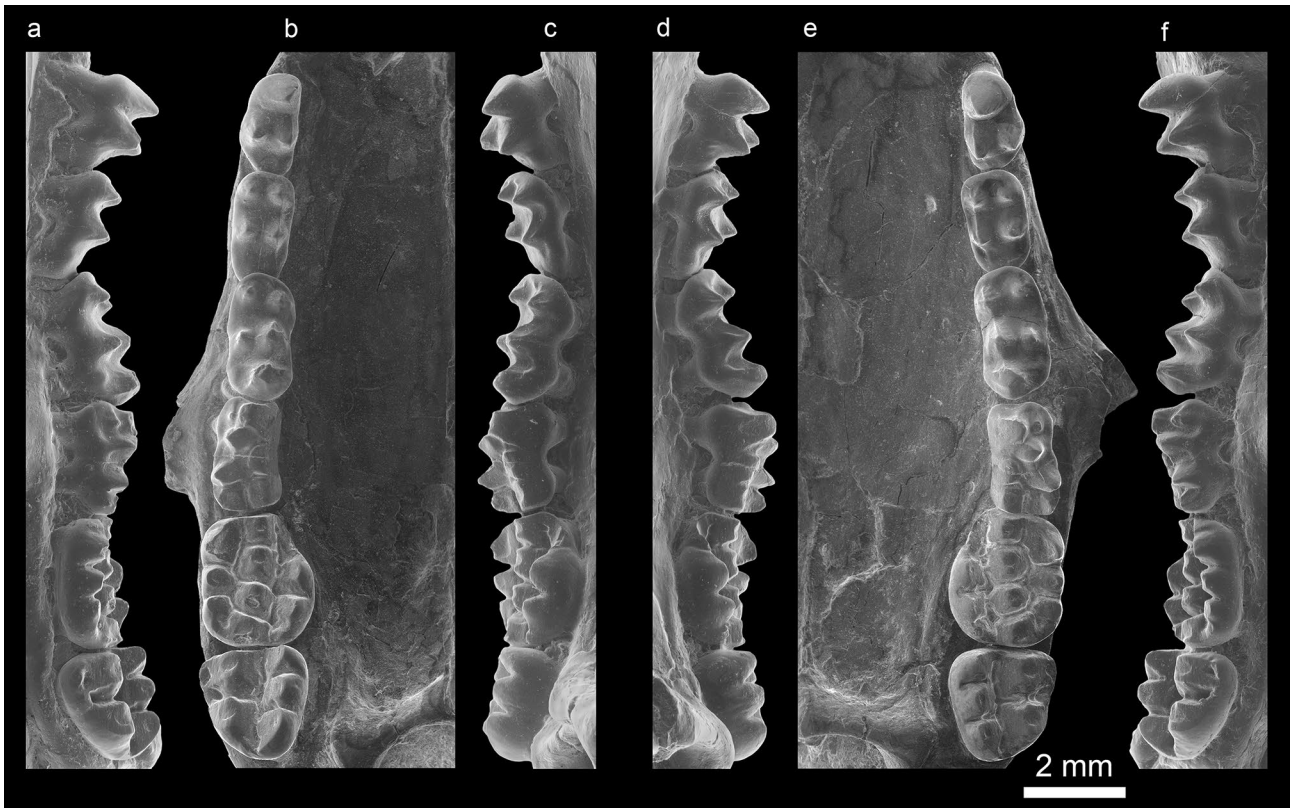

Fig. 5 Scanning electron micrographs of upper tooth rows of *Kogaionon radulescui*, sp. nov.. **a-c**, Right upper row with P1-M2 in labial (**a**), occlusal (**b**) and lingual (**c**) views. **d-f**, Left upper row with P1-M2 in labial (**f**), occlusal (**e**) and lingual (**d**) views

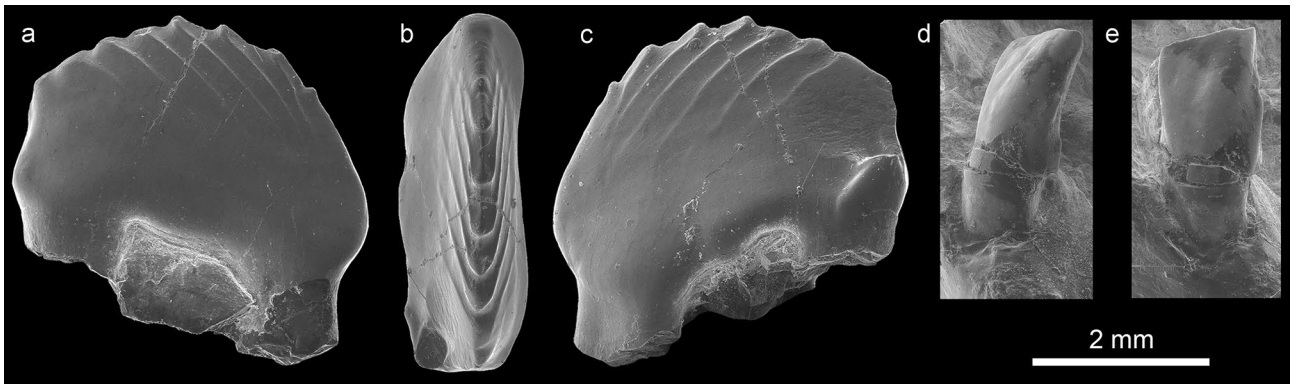

Fig. 6 Scanning electron micrographs of p4 (PSMUBB V-893b) and I3 of *Kogaionon radulescui*, sp. nov. **a-c**, Left p4 in lingual (**a**), occlusal (**b**), and labial (**c**) views. **d-e**, Right I3 in labial (**d**) and anterior (**e**) views

the two lingual cusps. The posterior crest of the posterolingual cusp extends beyond the cusp base somewhat on the flat posterior surface of P2.

The P3 bears five cusps, the cusp formula being 2:3 (Figs. 3, 5). As on P2, a small anterior cingulum joins the bases of the anterior labial and lingual cusps. All the cusps are well distinct, especially the labial ones. The latter are indeed more distant from each other than are the lingual ones (Fig. 5). The three lingual cusps are aligned in the anteroposterior axis of the tooth. The middle and posterior lingual cusps are larger than the other cusps of the tooth, the posterior one being also the highest. The posterolingual cusp also has a more rounded shape and is more worn than the middle one; the anterior-most cusp being not worn. Next to the posterolingual cusp, the posterolabial side of the tooth presents a small inclined and flat surface that does not bear a cusp. Few wrinkles are visible on the three cusps of the lingual row (Fig. 5). Thin anteroposterior crests are present on the cusps of the lingual row. They are in line with those on P1 and P2.

The P4 bears seven cusps, the cusp formula being 1:4:2 (Figs. 3, 5). A small cusp is present labially to the anterior-most cusp of the main (middle) cusp row, but it is very small on the right P4 (Fig. 5). The six other cusps are similar in size and distinct from each other with the cusps of the middle row arranged obliquely to the anteroposterior axis of the tooth. However, the two lingual cusps are more worn since they have a fairly rounded aspect. The same goes for the posterior-most middle cusp (Figs. 3, 5). The wear essentially affects the lingual side of all the cusps of the middle row and the occlusal side of the two lingual cusps.

The M1 bears ten cusps, the cusp formula being 3:4:3 (Figs. 3, 5). Most of the cusps are similar in size, except two. The anterolabial one is the largest cusp of the tooth, being about 1.5 times larger than the other ones. The smallest cusp is the posterolingual one, which is distinct on the left M1 but less clear on the right M1. Moreover, that cusp on the right M1 is almost fused with the one in front of it but this is possibly due to the wear of the posterior side of M1. A triangular, flat and narrow surface, with no cusp, is present on the anterolingual part of the tooth, anteriorly to the lingual row (Fig. 5). Small grooves, pits and ridges are visible between the cusps of the middle and lingual rows. Their weakness might be accentuated by the wear. In the valley, small ridges connect laterally the bases of some cusps. It is the case for the two middle cusps of the middle and lingual rows, as well as the most posterior cusps of the labial and middle rows (Fig. 5). The wear affects essentially the lingual side of the labial cusp row, the occlusal surface of the middle row, and the labial side of the lingual row. The posterior cusps are more worn than the anterior ones.

The M2 bears five cusps, the cusp formula being ridge:2:3 (Figs. 3, 5). The two middle cusps appear to be larger than the lingual ones and are joined together at their base by a small anteroposterior ridge (Fig. 5). The anterolabial edge of the tooth bears a worn external cingulum that connects the two middle cusps. A labiolingually oriented worn ridge connects the middle part of the external cingulum with the middle part of the anterior middle cusp (Figs. 3, 5). The wear strongly affects the occlusal surface of the middle cusp row and the labial side of the lingual row. Grooves, pits and ridges are strongly attenuated but still somewhat visible in the deepest part of the valley between labial and lingual cusp rows.

The i1 is long and slender with a slightly curved crown (Fig. 7a-c). The ventral part of the dentary is damaged, showing that i1 extends posteriorly beyond p4. The enamel covers the anterior part of i1. In lingual view, the enamel is restricted to a narrow band on the anterior side of the tooth. In labial view, the enamel covers much more the labial surface near the tip than near the root of the tooth.

The p4 is a high, blade-like tooth that presents an arcuate profile in lingual and labial views (Figs. 6a-c, 7a-c). It has two main rounded roots with possibly a third small

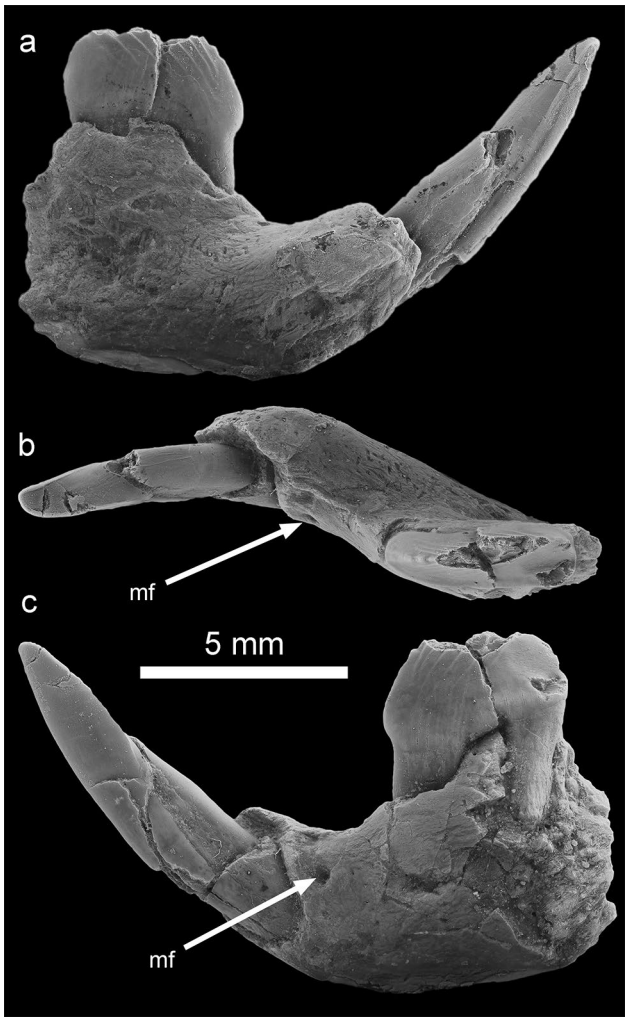

Fig. 7 Left dentary fragment UBB NV-Mt1 with i1 and p4 of *Kogaionon radulescui*, sp. nov., in lingual (**a**), occlusal (**b**), and labial (**c**) views. Abbreviation: mf, mental foramen

one centrally positioned between the other two roots. Anterior and posterior parts of p4 have about the same width in occlusal view. It bears eight small serrations and six ridges on both labial and lingual sides. A seventh short ridge might have been present on the labial side at the level of the eighth serration but hidden by the wear. A well-developed but worn, rounded cuspule is present on a short posterolabial platform (Fig. 6b, c); the platform, although well visible, is damaged in UBB NV-Mt1 (Fig. 7b-c). The anteroventral surface of p4 just above the anterior root is very short and rounded suggesting that no p3 was present. The absence of p3 is confirmed on the dentary fragment UBB NV-Mt1 (Fig. 7a-c).

Comparisons

The new partial mammal cranium associated with p4 and the dentary fragment with i1 and p4 from Nălaţ-Vad are referred to a cimolodontan multituberculate and, more specifically, to a small-sized kogaionid. Indeed, it presents the combination of the following typical characters: elongate snout with neurovascular foramina on the nasals placed far posteriorly; I2 placed close to I3, which is on the margin of the palatal part of the premaxilla; P1-3 strongly elongated, of which P3 is the longest; premolar row about twice as long as molar row; short and wide M1 with only four cusps in the middle row; and large, arcuate p4 (Rădulescu and Samson 1996, 1997; Kielan-Jaworowska and Hurum 2001; Csiki et al. 2005; Codrea et al. 2014; Smith and Codrea 2015; Solomon et al. 2016).

Comparison of the cranium bones of the new taxon with those of other kogaionids brings some new information. In dorsal view, the shape and proportions of the rostrum are similar to those of *K. ungureanui* whereas the rostrums of *B. transylvanicus* and *L. tholocephalos* are wider at the level of the anterior part of the maxillae (Fig. 8). The snouts of *K. ungureanui* and *K. radulescui* would possibly be the relatively longest and narrowest cimolodontan snouts known. The number and position of neurovascular foramina on the nasal are similar to those in *K. ungureanui* and *B. transylvanicus* (Fig. 8). The premaxilla seems a little less narrow labiolingually than in *K. ungureanui* but the left premaxilla of the latter has probably undergone a lateral compression at the level of the incisive foramen (Fig. 9a versus Fig. 9d). Like *K. ungureanui*, the posterodorsal process of the premaxilla is longer than in *B. transylvanicus*. The anterolateral edge of the incisive foramen is at the level of the anterior border of the I3 alveolus, as it is in *K. ungureanui* and *B. transylvanicus* (Fig. 9). The diastema between I2 and I3 in *K. radulescui* is similar to that of *K. ungureanui* and *L. tholocephalos* but a little longer than in specimen UBB P-Mt 1 of *B. transylvanicus*. The diastema between I3 and P1 is similar in length to that of *K. ungureanui*, *B. transylvanicus* and *L. tholocephalos* with the first half of diastema on the premaxilla and the second half, of similar size, on the maxilla. The infraorbital foramen is positioned at the level of the embrasure between P3 and P4 (Fig. 3c, e, f) as it is in *K. ungureanui* (see Csiki et al. 2018: suppl. fig. 4F), whereas it is at the level of the mid length of P3 in *B. transylvanicus* (see Smith and Codrea 2015, fig. 2) and *L. tholocephalos* (see Csiki-Sava et al. 2018: suppl. figs. 3F, G, 4F). The infraorbital foramen of kogaionids is positioned much more posteriorly than in taeniolabidoids and djadochtatherioids. An infraorbital foramen located posteriorly on the maxilla is also present in ptilodontoids and microcosmodontids. The sphenopalatine foramen is located above M1, as in *Microcosmodon* (Fox 2005), whereas it is located above M2 in *Tombaatar* and *Kryptobaatar* (Rougier et al. 1997; Wible and Rougier 2000). The sphenopalatine groove is deeper than in *Kryptobaatar*. The shape and size of the palatine is similar to that of *K. ungureanui* (Fig. 9a versus Fig. 9d) but

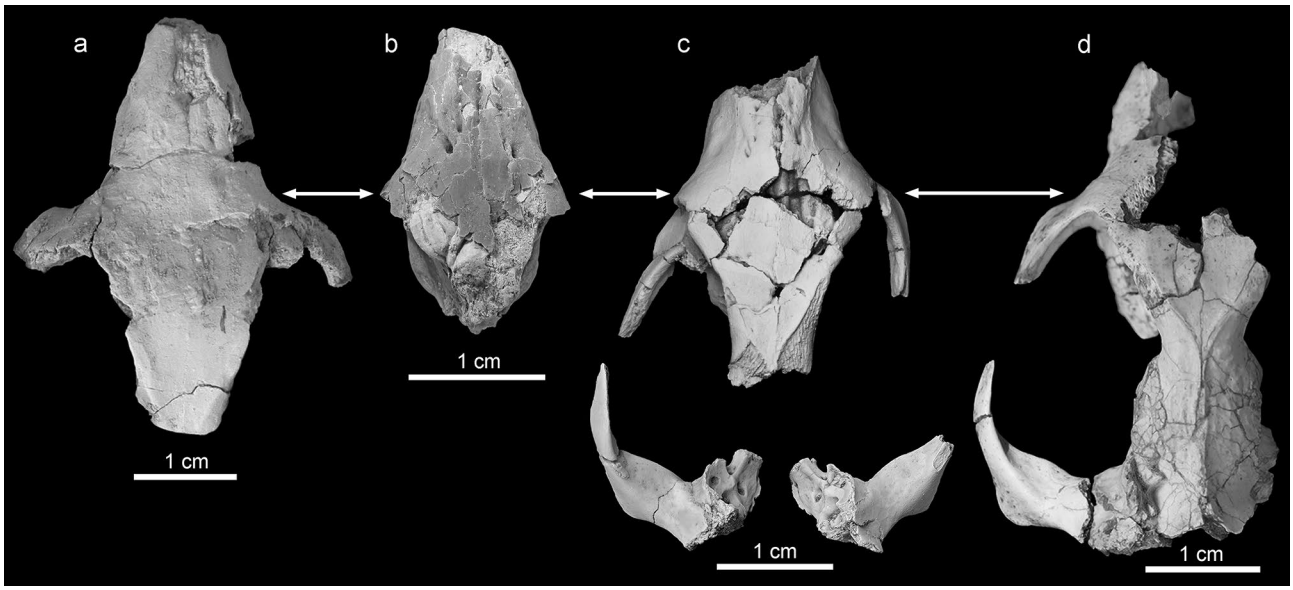

Fig. 8 Comparison of the partial skulls of kogaionids in dorsal views with the base of the snout set approximately at the same level as indicated by double-arrowed lines. **a**, *Kogaionon ungureanui*, ISB IS.001. **b**, *Kogaionon radulescui* sp. nov., PSMUBB V-893. **c**, *Barbatodon transylvanicus* UBB P-Mt 1 adapted from Smith and Codrea (2015). **d**, *B. transylvanicus* (=*Litovoi tholocephalos*), LPB (FGGUB) M.1700 adapted from Csiki-Sava et al. (2018)

the major palatine foramen is more difficult to locate than in the latter due to postmortem damage (Rădulescu and Samson 1996, 1997). The palatine is relatively similar to those of djadochtatherioids and differs from the large and long palatine of ptilodontoids and small and narrow palatine of taeniolabidoids (see Wible et al. 2019: fig. 22). It is located at the level of M1 as in djadochtatheriids and ptilodontoids whereas the palatine is at the level of M2 in taeniolabidoids. The morphology of the postpalatine torus is similar to that of *K. ungureanui*, although the latter is somewhat laterally compressed, giving it an inverted V shape (Fig. 9a). It resembles much that of *Microcosmodon* (Fox 2005: pl. 1, fig. 1). It is developed laterally and with a ventral projection from the palate forming a distinctive bulge as it is described in the djadochtatherioids *Catopsbaatar*, *Kryptobaatar*, *Chulsanbaatar*, *Kamptobaatar*, and *Nemegtbaatar* (Rougier et al. 2016). This morphology differs from the strongly developed postpalatine torus forming a raised, ornate, and sharply angled plate that is present in *Tombaatar*, *Mangasbaatar*, and *Guibaatar* (Rougier et al. 2016; Wible et al. 2019). The presence or absence of a postpalatine torus in the ptilodontoids *Ptilodus* and *Ectypodus* (Simpson 1937; Sloan 1979) and the taeniolabidoids *Taeniolabis* and *Lambdopsalis* is unclear (Rougier et al. 2016; Wible et al. 2019).

The well-preserved dentition of the new taxon facilitates enhanced comparisons with other kogaionids. The spatulate shape of I3 due to wear seems typical of kogaionids (see Smith and Codrea 2015: fig. 6A Csiki-Sava et al. 2018: fig. 1B: Solomon et al. 2021: fig. 3f, g). The very small bulge on its posterolabial side is also found in UBB P-Mt1 of *B. transylvanicus* (see Smith and Codrea 2015: fig. 6A). P1 is proportionally small and elongate, as in *K. ungureanui* and *B. oardaensis*, whereas P1 is much larger and bulbous in *B. transylvanicus* and *L. tholocephalos* (Fig. 10). The short, flat surface on its posterior side is a little longer than in *K. ungureanui* whereas this character seems absent or very weak in P1 of *B. transylvanicus* and *L. tholocephalos*. P2 has a long flat surface on its posterior side, as in *K. ungureanui*, *B. oardaensis*, and *H. belgica*. This surface is shorter in UBB P-Mt 1 of *B. transylvanicus* and LPB (FGGUB) M.1700 of *L. tholocephalos* (Fig. 10) but is variably developed at least in *B. transylvanicus* and *B. oardaensis* (Codrea et al. 2014: fig. 2B-C: Solomon et al. 2016: fig. 2B-D). P3 is slightly longer than P4, as in *B. oardaensis*, whereas P3 is much longer and larger than P4 in *B. transylvanicus* and *L. tholocephalos*. *Kogaionon ungureanui* seems to be intermediate morphologically, with P3 much longer than P4 but not as wide as in *B. transylvanicus* and *L. tholocephalos*. In *Hainina*, P3 has the same length as P4 based on isolated teeth (Fig. 10). Although P3 of *K. radulescui* is also very similar in shape and proportions to that of *B. oardaensis*, the latter differs in the presence of a third small cusp on the labial row (Fig. 10h, i). The anterior part of P4 is narrower or of nearly the same width as its posterior part, as in *K. ungureanui* and *B. oardaensis*, whereas the anterior part of P4 is wider than the posterior part in *B. transylvanicus* and *L. tholocephalos* (Fig. 10). The two latter species also have an inflated anterior-most cusp in the labial row of P4 with the three other

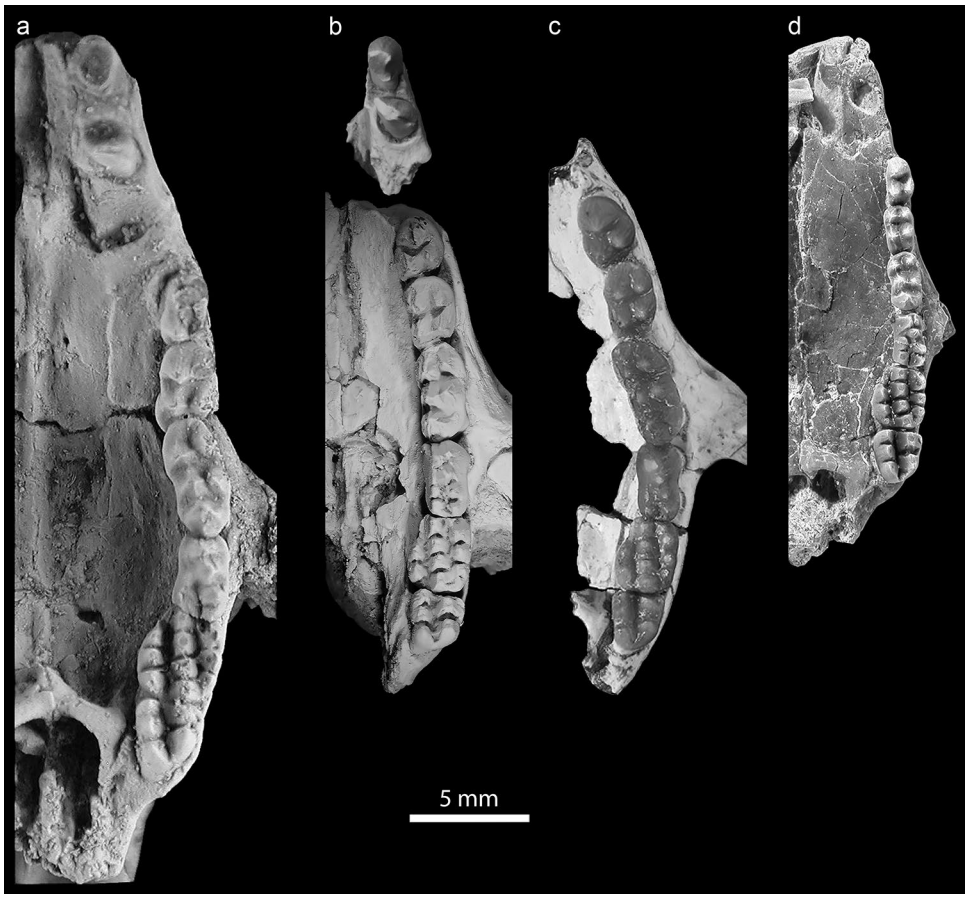

Fig. 9 Comparison of the left partial crania of kogaionids in ventral views. **a**, *Kogaionon ungureanui*, ISB IS.001. **b**, *Barbatodon transylvanicus*, UBB P-Mt 1. **c**, *B. transylvanicus* (=*Litovoi tholocephalos*), LPB (FGGUB) M.1700 adapted from Csiki-Sava et al. (2018). **d**, *Kogaionon radulescui*, sp. nov., PSMUBB V-893

cusps gradually decreasing in size towards the posterior side whereas the four cusps of the labial row are all of similar size and aspect in *K. radulescui*, *K. ungureanui*, and *B. oardaensis* (Rădulescu and Samson 1997; Codrea et al. 2014, 2017a; Solomon et al. 2021). The most anterior cusp in the labial row of P4 in *H. pyrenaica* is also the most developed cusp, followed by a second little smaller and lower cusp and then by a crest reaching the posterior edge of the tooth (Fig. 10q; Peláez-Campomanes et al. 2000). This combination of characters is similar to that of cf. *Hainina* sp. from the late Paleocene of Jibou-Rona, Romania (Gheerbrant et al. 1999). The cuspule present on the anterolabial part of P4 is variably developed on the left and right teeth in *K. radulescui* and seems also variably present in other species of kogaionids such as *B. transylvanicus* and *B. oardaensis*. M1 has a relatively square or rounded shape as in *K. ungureanui*, *B. oardaensis*, and *H. pyrenaica*, whereas it is sub-rectangular in *B. transylvanicus* and *L. tholocephalos* (Fig. 10: Smith and Codrea 2015: fig. 4: Solomon et al. 2016: fig. 2: Csiki-Sava et al. 2018; fig. 1E). It also has an anteroposteriorly longer lingual row with three cusps (the most posterior one being smaller and better visible in the left row), as in *K. ungureanui*. The lingual row is clearly shorter with only two cusps in *B. transylvanicus* and *L. tholocephalos* and a concave edge is present at the anterolingual part of the tooth (this edge is convex in other kogaionid species). *Barbatodon oardaensis* is morphologically intermediate for the length of the lingual row, which bears only two cusps. The labial row of *K. ungureanui* has three cusps as in most Maastrichtian kogaionids. A fourth cusp is sometime present in *B. transylvanicus* (UBB P-Mt2-7, Solomon et al. 2016: fig. 2G) and *L. tholocephalos*. M2 of *K. radulescui* does not differ significatively from that of other kogaionids except that it might be proportionally larger compared to M1. However, this needs confirmation by study of variability, which requires more specimens of that species. M1s and M2s are weakly ornamented with grooves, pits, and ridges, similar to those of *B. oardaensis*, whereas the ornamentation is stronger in *B. transylvanicus* (Solomon et al. 2016: Figs. 2-4) and even stronger in *H. godfriauxi* (De Bast and Smith 2017: fig. 6). The i1 of the dentary fragment UBB NV-Mt1 is similar in thickness to that of FGGUB M. 1635 and UBB P-Mt3-1 of *B. transylvanicus* (Csiki et al. 2005: Solomon et al. 2016). Only UBB P-Mt2 of the latter species presents a gracile i1 as noted by Solomon et al. (2016: 326); however, the i1 seems not completely erupted and UBB P-Mt2 could represent a young individual based on the very fresh p4-m2. The i1 of *K. radulescui* and *B. transylvanicus* is slenderer than in *Microcosmodon*, *Taeniolabis*, and some

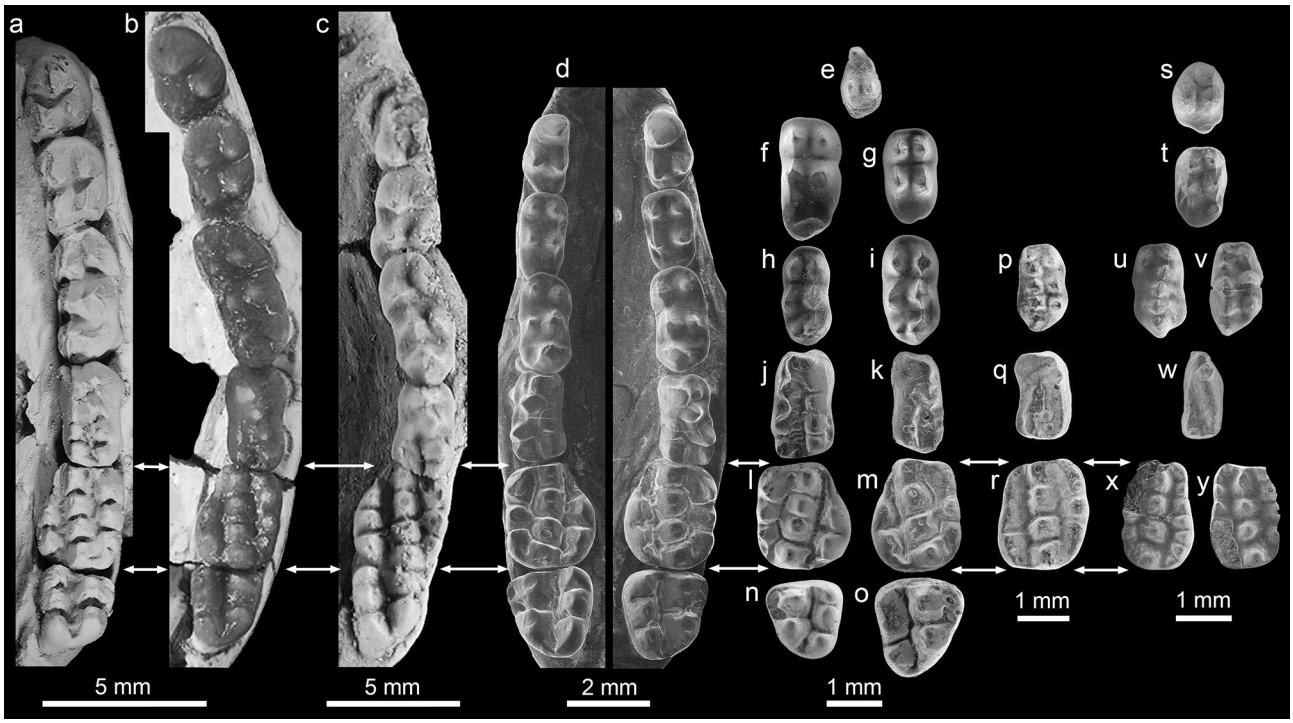

Fig. 10 Comparison of the upper dentitions of kogaionids in occlusal view with M1s scaled at the same length (as indicated by double-headed arrows). **a**, *Barbatodon transylvanicus*, UBB P-Mt 1. **b**, *B. transylvanicus* (= *Litovoi tholocephalos*), LPB (FGGUB) M.1700. **c**, *Kogaionon ungureanui*, ISB IS.001. **d**, *Kogaionon radulescui*, sp. nov., PSMUBB V-893. **e-o**, *Barbatodon oardaensis*, UBB ODAN-Mt-38, left P1 (**e**); UBBODAN-Mt-70, right P2 (**f**); UBB ODAN-Mt-71, right P2 (**g**); UBB ODAN-Mt-24, right P3 (**h**); UBB ODAN-Mt-69, right P3 (**i**); UBB ODAN-Mt-25, right P4 (**j**); UBB ODAN-Mt-21, left P4 (**k**); UBB ODAN-Mt-13, right M1 (**l**); UBB ODAN-Mt-7, left M1(**m**); UBB ODAN-Mt-67, right M2 (**n**); UBB ODAN-Mt-16, left M2 (**o**). **p-r**, *Hainina pyrenaica*, UCM FNT3-10, left P3 (**p**); UCM FNT3-2 left P4 (**q**); UCM FNT3-1 left M1 (**r**). **s-y**, *Hainina belgica*, IRSNB M1957, right P1 (**s**); IRSNB M1959, right P2 (**t**); IRSNB M1960, right P3 (**u**); IRSNB M2188, left P3 (**v**); IRSNB M2185, left P4 (**w**); IRSNB M1961, right M1 (**x**); IRSNB M2189, left M1 (**y**)

djadochtatherioids but more robust than in ptilodontoids. It is similar to *Pentacosmodon*, *Kryptobaatar*, and *Jeholbaatar*.

The p4 is similar in shape to those of other kogaionid p4s except that it is proportionally shorter anteroposteriorly and the crown is higher posteriorly (difference in height well visible between the posterior-most serration and the posterolabial cuspule in labial view) than in *B. transylvanicus* (Fig. 6 versus Smith and Codrea 2015: figs. 2I, J, L, 4F: Solomon et al. 2016: figs. 3, 4). In this sense, it resembles much the p4 of *B. oardaensis* (Codrea et al. 2014, fig. 2Q). However, it has a low number of serrations and ridges. *Kogaionon radulescui* has eight serrations and six ridges whereas *B. oardaensis* has 10 to 11 serrations and six to seven ridges (Codrea et al. 2014, 2017a; Solomon et al. 2021), *B. transylvanicus* 10 to 11 serrations and six to seven ridges (Solomon et al. 2016), and *H. belgica* 10 or 11 serrations and eight ridges (De Bast and Smith 2017). The width of p4 in occlusal view is similar to that of *Barbatodon* but differs from that of *Hainina*, which is much narrower posteriorly. The very short and rounded anteroventral surface of p4 just above the anterior root, suggesting the absence of p3, is also visible in *K. oardaensis* and *H. belgica*. The absence of p3 on the dentaries of *K. radulescui* and *B. transylvanicus* suggests that this character could be shared by all kogaionids.

Measurements of teeth indicate that, based on M1 average length, *K. radulescui* is about 35% smaller than *K. ungureanui*, about 20% smaller than *B. transylvanicus* and *L. tholocephalos*, and about 25% larger than *B. oardaensis*, *H. belgica*, and *H. pyrenaica* (Figs. 7, 9; Table 3; Supplementary Table S1). The ratio width/length of M1, a character established by Csiki-Sava et al. (2018), is relatively high in *K. radulescui*. It is 0.86 (mean of right and left M1s of PSMUBB V-893). This ratio is close to that of *K. ungureanui* which is 0.82 (ISB IS.001; Rădulescu and Samson 1996) and *B. oardaensis* which is 0.83 (mean of UBB ODAN-Mt-6 to 13, 65; Codrea et al. 2014 and UBB Vă-Mt-1; Solomon et al. 2021). The ratio is lower in *B. transylvanicus* with 0.76 (UBB P-Mt 1, 2–8, 3–4; Smith and Codrea 2015; table 1; Solomon et al. 2016; table 1) and even only 0.66 in *L. tholocephalos* (LPB (FGGUB) M.1700; Csiki-Sava et al. 2018: suppl. table S1). However, the ratio of the latter species goes back to 0.79 when calculated from fig. 1E of Csiki-Sava et al. (2018).

Another interesting ratio is P1-4/M1-2 length, a classic character in phylogenies, originally established by Kielan-Jaworowska and Hurum (1997). This ratio, which is high in kogaionids, is relatively low in *K. radulescui*. It is 1.80 (mean of right and left rows of PSMUBB V-893). This ratio is close to that of *B. oardaensis* which is 1.96, calculated by adding together the lengths of each isolated tooth (mean based on Codrea et al. 2014: table 2). This method is not accurate because several premolars slightly overlap each other in the maxilla. Therefore, it gives an overestimated ratio. By this method, the ratio is 2.37 in *K. ungureanui* (ISB IS.001; Rădulescu and Samson 1996) but only 2.15 based on direct measurements on the tooth row of Fig. 9. The ratio is 2.22 in *B. transylvanicus* (UBB P-Mt 1) and 2.53 in *L. tholocephalos* (LPB (FGGUB) M.1700) by adding all position length (2.45 based on direct measurements; Csiki-Sava et al. 2018: fig. 1).

Of even more potential interest is the proportional size of p4 relative to the molars. We cannot compare directly its length to that of m1, which is another classic character in multituberculates (Kielan-Jaworowska and Hurum 1997) because the latter is not preserved in PSMUBB V-893. However, by comparison with M1, which is almost comparable in length to that of m1, we see that the ratio of p4/M1 length is 1.64. This ratio is 1.77 for *B. oardaensis* (Codrea et al. 2014: table 2) and 1.82 (1.72 without the 15% smaller M1 IRSNB M2190) for *H. belgica* (De Bast and Smith 2017: table 2), whereas it is 2.34 for *B. transylvanicus* (Smith and Codrea 2015: table 1).

The strong morphological resemblance and the numerous characters shared between the new small kogaionid from Nălaţ-Vad and the type-species of the family Kogaionidae, *K. ungureanui*, allow us to erect the new species *K. radulescui*. Both are characterized by a long and narrow snout and share numerous characters, especially on P4 and M1. Compared to other Maastrichtian kogaionids, the morphology of *K. radulescui* is also closer to that of the very small *B. oardaensis*, thus potentially suggesting a close relationship between the two species. *Barbatodon transylvanicus* and *L. tholocephalos*, characterized by a wider snout, are the most different taxa from *K. radulescui*. The comparison of the morphological characters in kogaionids of different sizes allows also to analyze and rediscuss later in this paper these characters within the cimolodontans in order to better understand the evolution of the family.

Phylogenetic Analysis

Improvement for a More Accurate Phylogeny of Multituberculates

The 130 characters in the upgraded matrix have been scored for the following taxa: *Bryceomys*, *K. radulescui*, *B. oardaensis*, *H. belgica*, *H. pyreneica* (Supplementary Appendix S1).

In total, 113 modifications have been made to the phylogeny of Weaver et al. (2020). They are important as some erroneous scores persisted in the character matrices since Kielan-Jaworowska and Hurum's matrix (2001), 20 years ago (see Material and Methods for an overview on the history of these character matrices). Therefore, the modifications are here detailed and explained (Supplementary Appendix S2).

Character 7 (Angle between the lower margin of the dentary and alveolar line of the lower p4 and molars) has been changed from ? to 1 (18 degrees or above) for *B. transylvanicus* as it was scored by Smith and Codrea (2015). Indeed, when adding *B. transylvanicus* to the matrices of Xu et al. (2015) and Mao et al. (2016), Csiki-Sava et al. (2018) likely did not notice this modification even if this character state was already identified on the abundant available material (Csiki et al. 2005; Smith and Codrea 2015; Solomon et al. 2016). Character 7 has also been changed from 0 to 1 for *Microcosmodon* based on several complete dentaries figured by Fox (2005).

Character 16 (Enamel covering of lower incisor) has been changed from 1 (Thicker on labial surface than on lingual surface) to ? for *Boffius splendidus* because the large incisor, IRSNB M1955, originally identified by Vianey-Liaud (1979) has been transferred to *H. godfriauxi*, a species similar in size to *B. transylvanicus* (De Bast and Smith 2017). So, the lower incisor of *Boffius* is still unknown. This character was originally divided into three states (Kielan-Jaworowska and Hurum 2001) but successively reduced to two (Yuan et al. 2013) and then rescored in three states (Xu et al. 2015). However, during the last stage, *Glirodon* and *Microcosmodon* stayed scored at 1. We therefore rescored them 2 (Completely restricted to the labial surface of the tooth) as originally done by Kielan-Jaworowska and Hurum (2001). *Pentacosmodon* is here scored as 2 because Jepsen (1940: 322) mentioned in the diagnosis: "Lower incisor large, compressed laterally, enamel apparently limited, in the typical eucosmodontine pattern, to the lower border."

Character 17 (Number of upper incisors) has been changed from 2 (Two) to ? for *Boffius* as no upper incisors are known from that genus as correctly scored originally by Kielan-Jaworowska and Hurum (2001).

Character 18 (Diastema between Upper Incisor 2 and Incisor 3) has been changed from 1 (I2-I3 diastema) to 0 (No large diastema between the second and third upper incisors) for *Microcosmodon*, which has a short diastema (Fox 2005: 18, 26, pls. 1, 3) and for *K. ungureanui* and *L. tholocephalos* as, like other kogaionids, they do not have a large diastema between the two upper incisors (see Discussion).

Table 3 Summary measurements (in mm) for upper and lower teeth of different kogaionids. Raw measurements are given in Supplementary Tables S1 and S2. Abbreviations: L, length; W, width; M, mean; n, number of specimens; s, standard deviation

Species name		P1		P2		P3		P4		M1		M2		p4		m1		m2	
		L	W	L	W	L	W	L	W	L	W	L	W	L	W	L	W	L	W
Kogaionon ungureanui	M	3.20	1.85	4.20	2.20	5.00	2.25	3.70	2.15	3.90	3.20	2.90	2.70						
	n	1	1	1	1	1	1	1	1	1	1	1	1						
	s	-	-	-	-	-	-	-	-	-	-	-	-						
Barbatodon transylvanicus	M	2.78	2.23	3.71	2.26	4.20	2.10	3.64	2.03	3.75	2.84	2.53	2.38	8.10	2.30	3.42	2.30	2.30	2.32
	n	3	3	5	5	1	1	3	3	3	3	5	5	5	5	8	8	4	4
	s	0.19	0.18	0.42	0.14	-	-	0.24	0.09	0.40	0.25	0.19	0.15	0.45	0.10	0.31	0.15	0.36	0.22
Litovoi tholocephalos	M	3.55	2.32	3.77	2.02	4.95	2.32	3.69	1.93	3.52	2.33	2.79	2.33						
	n	1	1	1	1	1	1	1	1	1	1	2	2						
	s	-	-	-	-	-	-	-	-	-	-	0.01	0.01						
Hainina godfriauxi	M	2.40	1.72	2.26	1.81							2.23	2.06			2.70	1.90	1.80	0.97
	n	1	1	1	1							1	1			2	2	1	1
	s	-	-	-	-							-	-			0.03	0.01	-	-
Kogaionon radulescui	M	2.04	1.15	2.13	1.25	2.61	1.34	2.21	1.33	2.58	2.23	2.20	2.14	4.39	1.46				
	n	2	2	2	2	2	2	2	2	2	2	2	2	2	2				
	s	0.06	0.02	0.07	-	0.08	0.01	0.03	0.02	0.05	0.02	0.02	0.01	0.09	0.03				
Barbatodon oardaensis	M	1.20	0.91	2.02	1.02	1.92	1.02	1.80	1.04	1.88	1.56	1.51	1.44	3.55	1.06	2.06	1.33	1.23	1.33
	n	2	2	2	3	5	5	10	10	9	10	6	6	3	4	9	9	4	4
	s	-	0.2	0.14	0.05	0.09	0.16	0.15	0.10	0.11	0.11	0.23	0.17	0.21	0.12	0.11	0.1	0.03	0.09
Hainina pyrenaica	M	0.79	0.63			1.65	0.94	1,63	1,02	2.00	1.52					2.13	-	1.42	1.65
	n	2	2			2	2	1	1	1	1					1	-	1	1
	s	0.02	0.01			0.01	0.02	-	-	-	-					-	-	-	-
Hainina belgica	M	1.26	0.9	1.53	0.94	1.69	0.89	1.61	0.75	1.85	1.23			3.37	0.95	1.56	1.04	0.89	1.05
	n	3	3	2	2	3	3	1	1	3	5			1	1	2	2	1	1
	s	0.05	0.03	0.02	0.02	0.05	0.03	-	-	0.16	0.07			-	-	0.08	0.03	-	-

Character 19 (Upper Incisor 2 (or penultimate incisor) morphology) has been changed from 0 (Peg-like or single cusp) to ? for *K. ungureanui* because both I2s of the only known specimen are worn and the number of cusps is indeterminable. This erroneous score was already present in Kielan-Jaworowska and Hurum's matrix (2001). Csiki-Sava et al. (2018: suppl. p. 10) mentioned this issue with the I2 wear in *K. ungureanui* but did not modify the state in their matrix.

Character 20 (Upper Incisor 3 (or ultimate upper incisor) morphology) has been changed from 1 (2-cusped) to 0 (Single cusped or peg-like) for *K. ungurueanui* as its I3 presents a kind of bulge at the base but it is not a cusp strictly speaking. This bulge is also present in *K. radulescui* (Fig. 6d) and on some specimens of *B. transylvanicus*. Rădulescu and Samson (1997) previously indicated that I3 is peg-like in *K. ungureanui*.

Character 21 (Placement of posterior upper incisor (I3)) has been modified for several taxa. *Ptilodus* was scored 1 (Medial to the margin-crest of facio-palatal faces of premaxilla) while 0 (On the margin of premaxilla) is more correct (Simpson 1937: fig. 6). The same is observed for *K. ungureanui* whereas for *Lambdopsalis* it is the opposite as it was scored 0 instead of 1. *Stygimys* was scored 1 whereas 2 (More internal on the palatal part) is correct (Sloan and Van Valen 1965). The new scoring of character 21 is now the same as for character 9 in Rougier et al. (2016) and character 17 in Wible et al. (2019).

Character 28 (Cingular labial cuspules on posterior upper premolars) has been scored 0 (absent) for *Boffius* based on the identification of P3 and P4 cusp formula and their orientation in the upper jaw (De Bast and Smith 2017).

Character 29 (Upper premolars/upper molars length ratio) that is ordered has been changed from 3 to 0 (1.5 or more) for *B. transylvanicus* and *L. tholocephalos*. This fourth state scored 3 (2.2 or more) was originally added by Csiki-Sava et al. (2018) to accommodate the extremely elongated premolar tooth row in these two species. The results were not altered because Csiki-Sava et al. (2018) considered all the characters as unordered. However, this fourth character state does not exist anymore in the character list of Wang et al. (2019) and Weaver et al. (2020), whereas it persisted in the matrix.

Character 30 (Number and length of cusp rows of last upper premolar) has been scored 4 (One oblique main row

and one shorter, posteriorly placed lingual row) for *K. ungureanui*, as in Csiki-Sava et al. (2018), who added this fifth character state in order to accommodate all the kogaionids.

Character 32 (Width ratio of the ultimate upper premolar vs. M1) has been changed from 1 (0.9–0.7) to 2 (0.69–0.4) for *K. ungureanui* because its value is 0.67 (from Rădulescu and Samson 1996).

Character 36 (p3 (or penultimate lower premolar) laterally compressed to be blade-like) has been changed from 0 (No (including taxa with a peg-like p3)) to ? for *Pentacosomodon* because this genus has no p3 (Jepsen 1940).

Character 41 (Lower p4 (or ultimate lower premolar) laterally compressed to be blade-like) was scored 1 (Yes) for *Yubaatar* in Csiki-Sava et al. (2018) whereas it was originally 0 (No) in Xu et al. (2015). Later, Wang et al. (2019) and Weaver et al. (2020) rescored it 0. Therefore, we follow the original scoring 0.

Character 45 (Dorsal margin of p4 to m1) has been changed from 0 (On the level of molars) to 1 (Protruding dorsally over molars) for *B. transylvanicus* (Csiki et al. 2005: 77; Smith and Codrea 2015).

Character 48 (Ratio of p4:m1 length) has been changed from 2 (1.5–1.99) to 0 (Less than 0.99) for *Microcosmodon* (Jepsen 1940) and to 0/1 for *Catopsbaatar* (Wible et al. 2019). The erroneous score was accidentally done by Yuan et al. (2013) but later authors did not notice it. Importantly, this character was considered as ordered by Wang et al. (2019) and Weaver et al. (2020). However, we consider it as unordered because with the possible exception of ptilodontoids other groups of cimolodontans do not necessarily show an increase of p4 length by comparison with m1 length in their evolution. Moreover, recent results have shown that Early Cretaceous plagiaulacidan eobaatarids already had a long p4 relative to m1 (Kusuhashi et al. 2010, 2020).

Character 55 (M1 cusp formula) has been changed from 3 (5–11:7–10:6–11) to 4 (3–5:2–4:2–7) for *K. ungureanui* because we added a fifth character state, as Csiki-Sava et al. (2018: suppl. p. 45) did in order to accommodate the condition in kogaionids. The reason is that kogaionids do not fit with any of the three previous character states. Like Csiki-Sava et al. (2018), we consider this character as unordered, a situation differing from Wang et al. (2019) and Weaver et al. (2020).

Character 58 (M1 posterolingual wing to M1 length) has been changed from 0 (Present and below 0.2) to 1 (Present and between 0.2 and 0.5) for *Kryptobaatar*. This genus has indeed a posterolingual wing that is nearly half of the M1 length (Kielan-Jaworowska and Hurum 2001; Kielan-Jaworowska et al. 2003).

Character 66 (M2 mesiobuccal ridge: (0) Absent; (1) Present; (2) Present and expanded to mesial margin of labial cusp row) has been changed from 1/2 to 1 for *Litovoi*. Character state 2 has been originally accommodated for some plagiaulacidans such as *Rugosodon* and *Kuehneodon* that have the mesiobuccal ridge forming a particular anterior structure (see Yuan et al. 2013: suppl. fig. S2A-B). The M2 mesiobuccal ridge in LPB (FGGUB) M.1700 of *Litovoi* is similar to that of other *B. transylvanicus* M2s (Smith and Codrea 2015: fig. 4B, C: Solomon et al. 2016: fig. K, M) and is not expanded to the mesial margin of the labial cusp row.

Character 67 (m1 main lingual cusp count) has been changed from 2 (6 or higher) to 0/1 (4 or fewer or 5) for *Microcosmodon* (Fox 2005). This character, which was originally scored based on the two rows of m1 (Kielan-Jaworowska and Hurum 2001), was erroneously revised by Yuan et al. (2013). The m1 of *Microcosmodon* indeed has 4–5 cusps on the lingual row, whereas it has 7–8 cusps on the labial row (see Fox 2005: 40).

Character 76 (Molar enamel surface) has been changed from 0 (Not ornamented) to 1 (Covered with grooves, pits, and ridges) for *B. transylvanicus* and *L. tholocephalos*, which have obviously ornamented molars (Smith and Codrea 2015: fig. 4: Solomon et al. 2016: fig. 2: Csiki-Sava et al. 2018: suppl. fig. 4B). This character can be variable for *Hainina*. While the molars of *H. belgica* seem to have smooth enamel, those of *H. godfriauxi* are strongly covered with grooves, pits, and ridges (Vianey-Liaud 1979; De Bast and Smith 2017). The character has been scored 0/1 for *H. pyrenaica*, *B. oardaensis*, and *K. radulescui* as these species have ornamented molars but some specimens seem not or weakly covered with grooves, pits and ridges. Nevertheless, this character remains difficult to establish because sometimes even weak wear is enough to attenuate the ornamentation on the molars. *Kogaionon ungureanui* has been scored 0 but based on the wear of the molar cusps it cannot be excluded that this is an artefact, especially as some ridges connecting cusps are still visible.

Character 77 (Enamel microstructure) has been changed from ? to 1 (Gigantoprismatic) for *K. ungureanui* because this character state was identified by Fosse et al. (2001). This correction had been already modified in Smith and Codrea (2015); however, later authors followed the original matrix of Yuan et al. (2013), which did not contain this information.

Character 82 of Weaver et al. (2020) (Sharp ridge between the palate and lateral walls of premaxilla: (0) Absent; (1) Present) was already present in the matrix of Yuan et al. (2013) and corresponds to character 40 of Kielan-Jaworowska and Hurum (2001). Originally, this character was specifically scored for Djadochtatherioidea in which this sharp ridge between the lateral and palatal walls of premaxilla is a synapomorphy of that superfamily (Kielan-Jaworowska and Hurum 1997). However, Yuan et al. (2013) scored 2 all of the Djadochtatherioidea and *Pentacosmodon*, but this score does not exist for that character since it has only two states. They also scored 1 for *Glirodon*, *Meniscoessus*, *Ptilodus*, *Microcosmodon*, *Taeniolabis*,

Lambdopsalis, *Kogaionon*, and *Stygimys* instead of 0 for the seven former and ? for the latter as originally scored by Kielan-Jaworowska and Hurum (2001) or illustrated later by Fox (2005) for *Microcosmodon*. *Sinobaatar* was added to the matrix and scored 1 as well (Yuan et al. 2013), whereas no sharp ridge was observable in *Sinobaatar* (Kusuhashi et al. 2009). These erroneous scores were repeated by all later authors who used Yuan et al.'s matrix (2013). Later Xu et al. (2015) added *Sphenopsalis*, *Prionessus*, and their new genus *Yubaatar*, which were all scored 1. However, no premaxilla is preserved for *Yubaatar*, so it is not possible to identify whether the ridge is present or not in this genus. Mao et al. (2016) also kept the scores of Xu et al. (2015) whereas they figured a partial rostrum with I2-3 of *Sphenopsalis nobilis*, IVPP V19025, that clearly shows that no sharp ridge is present between the palate and lateral walls of the premaxilla. Therefore, we used the original scoring of character 40 of Kielan-Jaworowska and Hurum (2001), similarly as done recently by Rougier et al. (2016: character 19) and Wible et al. (2019: character 45) to which we applied modifications for the taxa that were later added to Kielan-Jaworowska and Hurum's matrix: *Sinobaatar* and *Sphenopsalis* are now scored 0 while *Prionessus* and *Yubaatar* are scored.

Character 83 (Curvature of anterior zygomatic root) has been changed from 2 to 0 (Zygomatic root aligned with facial part of rostrum) for *Ectypodus*, *Catopsbaatar*, and *Kryptobaatar*. Indeed, Yuan et al. (2013) reduced the number of states for this character, which was originally defined by Kielan-Jaworowska and Hurum (2001) as character 41. However, the score was not modified for these tree taxa. Later authors followed the matrix of Yuan et al. (2013) containing these unmodified scores.

Character 84 (Number of pairs of vascular foramina on nasal) has been changed from 4 to 3 (Three or more) for *Yubaatar* (Xu et al. 2015) because Wang et al. (2019) scored it 4 whereas this state does not exist for that character. Weaver et al. (2020) still used this erroneous score.

Character 93 (Facial exposure of lacrimal) and character 94 (Thickening in palatal process of premaxilla) have been changed from 1 (Large, roughly rectangular) and 1 (Present) respectively to ? for *Rugosodon* (Yuan et al. 2013) because these characters cannot be determined due to the broken skull as correctly scored in the character list of Yuan et al. (2013: 107). However, Yuan et al. (2013: 109) erroneously scored 1 in the character matrix, which was repeated by all later authors who did not notice it.

Characters 112 (Mandibular condyle, size, relative to mandible size: (0) Large; (1) Small) and 113 (Mandibular condyle, orientation: (0) Facing posteriorly; (1) Facing dorsoposteriorly) have been changed from ? to 0 for *Microcosmodon*, which has been well figured by Fox (2005: pl. 4).

Character 116 (Upper incisor 3 form) has been changed from 0 (conical) to 2 (Transversely wide and anteroposteriorly compressed) for *K. ungureanui* and from ? to 2 for *B. transylvanicus* and *Litovoi* because the shape of I3 is known for the three taxa (fig. 7: Csiki-Sava et al. 2018: fig. 1). The state has also been changed from ? to 0 for *Prionessus* that has been figured by Mao et al. (2016: fig. 3).

Character 125 (Penultimate upper premolar, outline) has been changed from 0 (Triangular or square) to 1 (Rectangular with length greater than width) for *Boffius* based on the identification of the P3 shape (De Bast and Smith 2017).

Character 126 (Ultimate upper premolar: the length to width ratio) has been changed from 1 (1.4–1.7) to 2 (> 1.7) for *K. ungureanui* (ratio 1.72 from Rădulescu and Samson 1997), *B. transylvanicus* (ratio between 1.73 and 1.82 from Smith and Codrea 2015; Solomon et al. 2016), and *Litovoi* (ratio 1.91 from Csiki-Sava et al. 2018).

Character 127 (Ultimate upper premolar: main cusp row count) has been changed from ? to 1 (5–8) for *Boffius* and *Buginbaatar* based on the identification of six cusps in the main row (Kielan-Jaworowska and Sochava 1969; De Bast and Smith 2017).

Character 129 (Upper premolar enamel surface) has been changed from 0 (Not ornamented) to 1 (Ornamented with ridges) for *Litovoi* and *B. transylvanicus* (fig. 9).

Finally, 23 other character states have been changed for *Pentacosmodon* based on the study of Fox (2005), and 22 character states have been changed for the eobaatarid genera *Sinobaatar*, *Heishanobaatar*, *Liaobaatar*, and *Hakusanobaatar* based on the recent study of Kusuhashi et al. (2020).

Despite numerous character states having been revised, we cannot exclude that other further modifications might be necessary for other erroneous scores or bibliographic references that we would have missed. In addition, some characters should probably be revised (e.g., characters 31 and 127 that may be redundant in cimolodontans; character 119 that is restricted to *Taeniolabis* and *Catopsalis* but not present in all species of both genera (see Williamson et al. 2016 for the original description).

Analysis with the New Character Matrix

The strict consensus tree (Supplementary Fig. S1) is quite well resolved regarding the taxon of interest and its close relatives. However, the basal plagiaulacidan taxa and *Thomasia* and *Haramiyavia* form a polytomy, as well as the Eobaataridae. The Kogaionidae form the most basal clade within the Cimolodonta, after *Bryceomys*. Together, they emerge between the Eobaataridae and the Taeniolabidoidea. The majority-rule consensus tree (Fig. 11) shows the same results, except for the two polytomies that are fully resolved. Only the Djadochtatherioidea are not monophyletic, the Eucosmodontidae, *Boffius* and *Buginbaatar* being part of them. The Eucosmodontidae and *Buginbaatar* are often close to the Djadochtatherioidea in

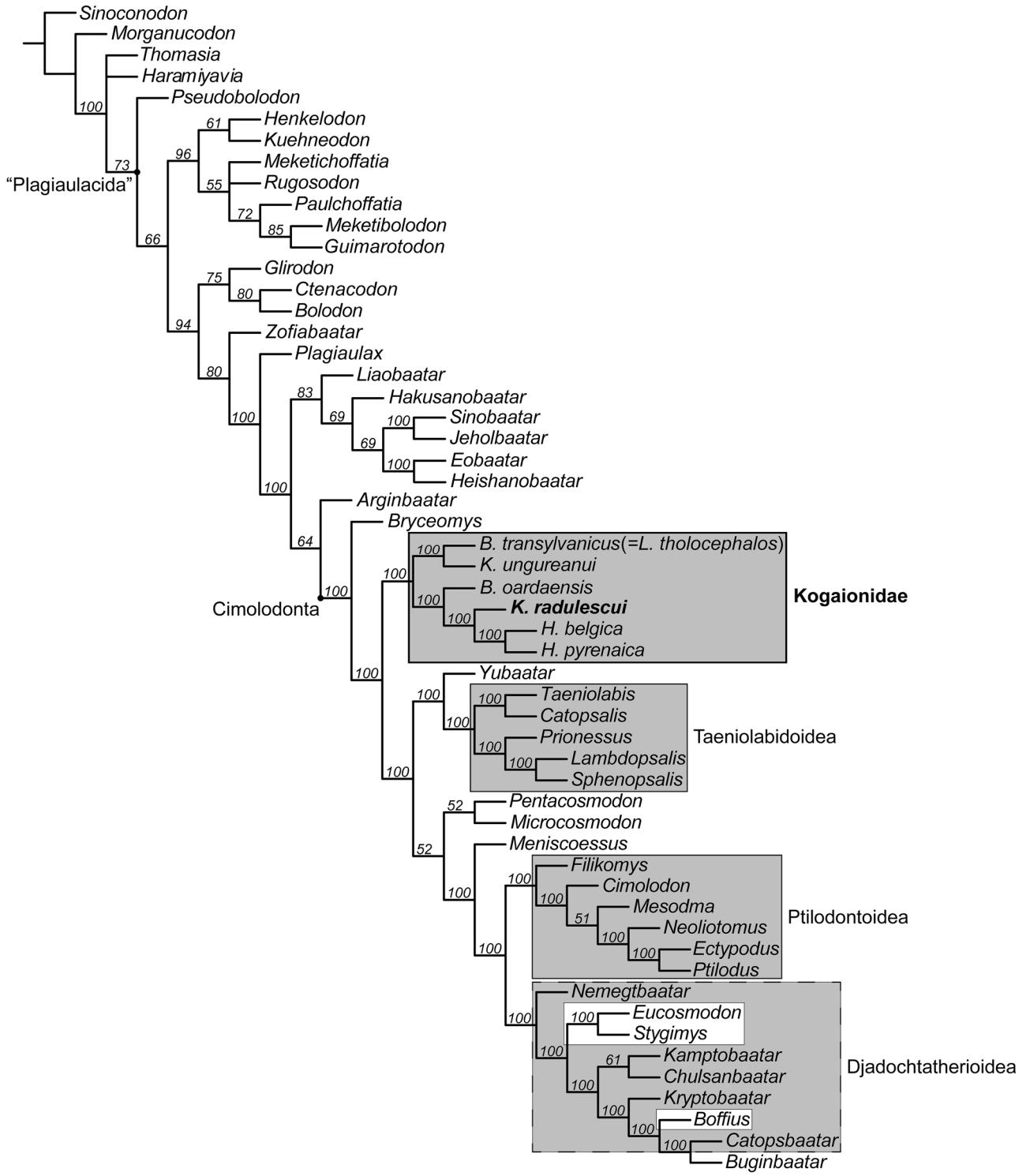

Fig. 11 Majority-rule consensus cladogram of the 3325 equally most parsimonious trees resulting from the analysis based on the updated matrix. Tree length = 481; CI = 0.418; RI = 0.762

different cladistic analyses, whereas *Boffius* is labile and its position in the tree varies from one cladistic analysis to another (e.g., Smith and Codrea 2015; Csiki-Sava et al. 2018; Weaver et al. 2020). Compared to the tree in Smith and Codrea (2015), Ptilodontoidea and Djadochtatherioidea are sister taxa and *Microcosmodon* and *Pentacosmodon*, traditionally considered members of the same family, actually group together.

The Kogaionidae appear to be the sister taxa of all other cimolodontans considered in the phylogeny, except *Bryceomys*. The advantage of scoring species of *Hainina*, including the type-species *H. belgica*, is that it allows for the first time to polarize the tree for kogaionids. Indeed, the teeth of *Hainina* are more complex with a higher number of cusps in rows of several dental positions. Moreover, *Hainina* comes from Paleocene deposits, respectively early Danian for *H. pyrenaica* (Peláez-Campomanes et al. 2000) and late Danian for *H. belgica* (De Bast and Smith 2017). Within the Kogaionidae, two clades appear. One is formed by the Maastrichtian *K. ungureanui* and *B. transylvanicus* – *L. tholocephalos*. The second is formed by the Maastrichtian *B. oardaensis*, from which emerge successively *K. radulescui* and the most derived kogaionids, the Paleocene *H. belgica* and *H. pyrenaica*.

Although the tree is relatively well resolved with the five additional taxa, the 113 modifications and characters 48 and 55 considered unordered, we performed some tests in order to estimate if it can be further improved. First, considering character 48 (Ratio of p4:m1 length) ordered does not change the results within the cimolodontans and only slightly changes the position of *Meketichoffatia* within the basal plagiaulacidans. This suggests that the progressive increase in size of p4 is only restricted to some groups such as plagiaulacids and ptilodontoids and is not a general tendency of multituberculates (see Discussion below). Therefore, character 48 is better unordered. Second, considering character 55 (M1 cusp formula) ordered changes the position of *Boffius*, which fits outside djadochtatherioids and ptilodontoids; *Arginbaatar* fits basal to eobaatarids; and, most djadochtatherioids then appear in a polytomy. This test suggests that character 55 should probably be divided into several characters with at least one ordered for the number of cusps on M1 middle row, the labial and lingual cusp rows varying independently from the middle row. Moreover, the unstable positions of *Boffius* and *Arginbaatar* witness a lack of knowledge of these two particular multituberculates. Third, analyzing only the first 107 characters, without the 23 characters added by Wang et al. (2019), does not change the results for cimolodontans except for kogaionids and the most derived plagiaulacidans, especially eobaatarids. This confirms the usefulness of the characters of Wang et al. (2019) regarding eobaatarids and also suggests their usefulness for the plagiaulacidan-cimolodontan transition, which has been, until now, not well understood.

Discussion

Importance of the New Specimens

The cranium from Nălaţ-Vad is the first known for a small-sized kogaionid. It is also the second specimen found of *Kogaionon*, the type genus of the family. When still embedded in the marl matrix, it was associated with a left p4 located next to the right upper tooth row (Fig. 2). This p4 is here considered as belonging to the same individual as the cranium for several reasons. First, the p4 has the expected size for the upper tooth row size. Second, the tooth is in the same anteroposterior orientation as the upper tooth row with the anterior part at the levels of the P2s and the posterior part at the level of the P3s. Third, the p4 is only little worn, like the upper corresponding teeth. Fourth, the p4 and cranium were found together in a floodplain deposit where the specimens are disseminated on several thousands of square meters (Van Itterbeeck et al. 2004, 2005), making a fortuitous gathering practically improbable.

Although p4 is next to the right P2-3, it is not a right tooth, indicating that it was slightly displaced from the left to the right side of the cranium before fossilization. The roots of p4 show fresh breaks, suggesting that the rest of the left dentary might have been associated with the cranium before discovery.

The discovery of p4 associated with the new cranium allows identification of the morphology of this tooth position in the genus *Kogaionon* for the first time. Until now, among kogaionids, only *Barbatodon* was known from lower and upper teeth in direct association (Csiki et al. 2005; Smith and Codrea 2015; Solomon et al. 2016). Although very similar in shape to other p4s of kogaionids, the p4 of *K. radulescui* is relatively short and high, like that of *B. oardaensis*, whereas it is proportionally much longer in *B. transylvanicus*. *Kogaionon radulescui* is characterized by a lower number of serrations and ridges than any other kogaionid species known to date, including *B. oardaensis*, suggesting, once again, that the number of serrations and ridges is variable in kogaionids as in other families.

The dentary fragment confirms the low number of ridges on p4, the absence of p3, and allows identification of i1 in the genus *Kogaionon* for the first time.

Synonymy Among Kogaionids

Morphological study of the new small cranium and the dentary fragment, based on bones and dentition, indicates that they belong to a new species of *Kogaionon*. This species, *K. radulescui*, allows better definition of the characters of the genus *Kogaionon* and for distinguishing it from the genus *Barbatodon*. *Kogaionon* differs from *Barbatodon* in its narrower snout, proportionally smaller P1, narrower anterior part of P4 with four similar-sized cusps in the middle row, and a more squared or rounded M1 with an anteroposteriorly longer lingual row. Most of these characters are also present in the small species *B. oardaensis*. However, the latter presents only two cusps in the lingual row of M1, as

in *B. transylvanicus* (plesiomorphic condition) and a small P3 (apomorphic condition), making this species morphologically intermediate between *B. transylvanicus* and *K. radulescui*.

Our study also highlights how much *L. tholocephalos* is similar to *B. transylvanicus*. Like the latter, *L. tholocephalos* is a large-sized kogaionid found in the same locality and stratigraphic level. Csiki-Sava et al. (2018) considered the two species to be sympatric. One can question if *L. tholocephalos* would be synonymous with *B. transylvanicus* or, if it is recognized as a different species from *B. transylvanicus*, would it belong at least to the genus *Barbatodon*. It is indeed peculiar to have two different species and, even more, two different genera for specimens so close morphologically, phylogenetically, in size, and occurring contemporaneously at the same place. The only case of sympatry known from the Haţeg Basin is the abundant rhabdodontid iguanodontian dinosaur *Zalmoxes* for which two species are distinguished from each other based on a series of autapomorphical characters (Godefroit et al. 2009).

Lithovoi tholocephalos has been diagnosed by "an autapomorphically vaulted skull roof with the highest point of the arch at the level of the supraorbital notch, as well as a unique combination of characters: very elongated upper postcanine tooth row with apomorphically elongated P1 and P2, an elongated P3 having a cusp formula of 2:5, and an inflated first labial cusp on P4" (Csiki-Sava et al. 2018: 2). Except for the vaulted skull roof and the cusp formula of P3, all of these characters are the same as those of *B. transylvanicus*. Next to those, several other characters are shared only by these two taxa relative to other kogaionids: wider snout anteriorly, much larger P1, wider anterior part of P4, and more rectangular M1. Nevertheless, seven features in total have been invoked to discriminate *L. tholocephalos* from *B. transylvanicus* (Csiki-Sava et al. 2018: suppl. p. 15). We analyze each of them here in review to check their relevance and test the validity of the genus *Litovoi*.

(**1**) *The larger body size*. M1 of *L. tholocephalos* is about 10% longer than that of UBB P-Mt-1 of *B. transylvanicus* (Csiki-Sava et al. 2018). The authors recognize that this size difference may appear marginal (Csiki-Sava et al. 2018: suppl. p. 15) but that the femur of LPB (FGGUB) M.1700 is about 24% longer than a femur recovered with LPB (FGGUB) M.1635 of *B. transylvanicus* (Csiki et al. 2005). Following the authors this suggests that the body proportions of *L. tholocephalos* were probably also somewhat different from those of *B. transylvanicus*. While the identification of the femur LPB (FGGUB) M.1635 cannot be discussed here because it is undescribed, we can at least discuss the size variability in kogaionids and other families of multituberculates. *Barbatodon transylvanicus* is not rare at the Pui locality, with different specimens having been discovered on a surface of a few hundred square meters since early 1980s and with a size variability of 18–25% based on lower and upper molars (Solomon et al. 2016: table 1). This variability in size may appear important but is however totally comparable with the variability based on m1 and M1 of numerous species of multituberculates for which sufficient material is available. This variability is indeed similar to what is observed in the kogaionid *B. oardaensis* from the Maastrichtian of Oarda de Jos in Romania (Codrea et al. 2014: table 1), the ptilodontoid *Filikomys primaevus* from the late Campanian Egg Mountain in Montana (Weaver et al. 2020: suppl. table S5), the ptilodontids *Ptilodus mediaevus* from the early Paleocene Swain Quarry in Wyoming (Rigby 1980: table 9), and *Ptilodus kummae* and *Prochetodon foxi* from the late Paleocene Roche Percée UAR2a locality in Saskatchewan (Krause 1977: table 1, 1987: table 1), the microcosmodontid *Microcrosmodon rosei* from latest Paleocene SC-188 in Wyoming (Krause 1980: table 6), and the neoplagiaulacids *Neoplagiaulax nicolai* and *N. copei* from the late Paleocene of Cernay in France (Vianey-Liaud 1986: 112) and *Mimetodon silberlingi* from the late Paleocene Roche Percée UAR2a locality in Saskatchewan (Krause 1977: table 16) and *Paraectypodus lunatus* from the early Eocene East Alheit Pocket Quarry, Four Mile Creek, Colorado (Krause 1982a: table 7).

(**2**) *The autapomorphically vaulted skull*. *Litovoi tholocephalos* would differ from *B. transylvanicus* by the autapomorphically marked inflection of the skull roof at the level of the anterior part of the frontal, above the orbital region, giving the skull of *Litovoi* its domed shape (Csiki-Sava et al. 2018). However, Krause et al. (2020: suppl. p. 30) remarked that "the cranium in the type and only specimen of *Litovoi tholocephalos* is comprised of four fragments that do not actually contact. The distance between the cranial roof fragments, although estimated at only 1 mm, could impact the degree of doming and possibly the estimate of cranial length.". We agree with Krause et al. (2020) that the reconstruction of LPB (FGGUB) M.1700 does not seem natural. The assemblage of the different broken fragments exaggerates the angle between the tooth row and the occipital region in lateral view (see Csiki-Sava et al. 2018: suppl. fig. 4H). Moreover, the autapomorphically vaulted skull roof of *L. tholocephalos* claimed by the authors is not correct as *Kogaionon* also has a vaulted skull roof (see Csiki-Sava et al. 2018: suppl. fig. 4H), even if it is to a lesser degree than reconstructed for *L. tholocephalos*. In fact, none of the skulls are complete and both are subject to some deformation. The partial skull of *B. transylvanicus* (Smith and Codrea 2015) does not preserve the braincase and therefore does not allow us to describe correctly the skull roof. Therefore, the reconstruction of that part was done like in most other multituberculate families (e.g. relatively flat skull roof). So, we hypothesize, based on *Kogaionon* and *Litovoi*, that the vaulted skull roof is a synapomorphy of kogaionids.

(**3**) *The presence of a relatively longer diastema between I2 and I3*. Based on character 18 of Csiki-Sava et al. (2018), *L. tholocephalos* shares with *K. ungureanui* a I2-I3 diastema (character state 1) whereas *B. transylvanicus* has no large diastema between I2 and I3 (character state 0). Our study contradicts this statement and shows that the two former taxa share with *B. transylvanicus* a similar diastema length between I2 and I3 (Fig. 9b). Moreover, a certain variability of the diastema length must exist. In any case, the new *K. radulescui* also has a similar diastema size between I2 and I3 (Figs. 4b, 9d). The difference we see is that the diastema in both *K. ungureanui* and *K. radulescui* is a little longer than in both *B. transylvanicus* and *L. tholocephalos*. A diastema between I2 and I3 is indeed present in all kogaionids but relatively short by comparison with the diastema visible in numerous other multituberculates such as the cimolomyid *Meniscoessus* (Archibald 1982), eucosmodontid *Stygimys* (Sloan and Van Valen 1965: fig. 4), the ptilodontoids *Ptilodus* and *Filikomys* (Simpson 1937: fig. 6: Weaver et al. 2020: fig. 1) and djadochtatherioids (Wible et al. 2019: fig. 22). It is closer to the length seen in the eobaatarid *Sinobaatar* (Kusuhashi et al. 2009: figs. 5, 14), although a little shorter.

(**4**) *A sinuous instead of rectilinear postcanine tooth row in occlusal view, with the P3 oriented clearly labio-distally relative to the rest of the upper teeth*. Despite that the maxilla of *L. tholocephalos* is broken between P4 and M1 and between M1 and M2 (Csiki-Sava et al. 2018: fig. 1E) and that the skulls LPB (FGGUB) M.1700 and UBB P-Mt-1 from Pui are both a little deformed, the sinuous postcanine tooth row mentioned by the authors is indeed visible, a character that they consider as shared with *K. ungureanui*. However, Fig. 9a clearly shows a more rectilinear tooth row in *K. ungurenui* than originally drawn by Rădulescu and Samson (1996: figs. 1, 2), the angle of this curvature also depending on the orientation view. This orientation is similar to Fig. 9d of *K. radulescui*. The undeformed postcanine tooth rows of *K. radulescui* allow the observation that, in labial view, the row is not straight but forms two curves with an inflexion point at the level of the anterior part of P4 (fig. 4D). This is also clearly visible in *B. transylvanicus*, *K. ungureanui*, and *L. tholocephalos* (Smith and Codrea 2015: fig. 1C: Csiki-Sava et al. 2018: suppl. figs. 4F, H) and therefore is here considered as a character shared by all kogaionids. It is probably a common feature of multituberculates with long upper premolar rows and short upper molar rows, due to occlusion with a large p4 such as is also the case in the ptilodontids *Prochetodon* and *Ptilodus* (Krause 1980: text-fig. 3, 1982b: fig. 6, 1987: fig. 3). Regarding the labiodistally oriented P3 in LPB (FGGUB) M.1700, we interpret it as an insignificant abnormality that is probably part of the variability (tooth slightly rotated counterclockwise in occlusal view) because the anterior part of P3 is not in line with the flat posterior surface of P2 whereas the posterior part of P3 is in line with P4. In addition, P3 and P4 should occlude with p4 and thus probably originally formed together a relatively flat lingual cutting surface.

(**5**) *Relatively more elongate P2 and P3*. These dental positions would be proportionally almost 20% longer in *L. tholocephalos* than in *B. transylvanicus* (Csiki-Sava et al. 2018). We agree that P3 is relatively long in LPB (FGGUB) M.1700, however P2 is not. P2 of LPB (FGGUB) M.1700 fits into the size range of *B. transylvanicus* (Table 3; Solomon et al. 2016: table 1). The size range of P3 is unknown in *B. transylvanicus* as this position is known only in UBB P-Mt-1. The only kogaionid that provides data for P3 variability is *B. oardaensis*, indicating, based on the available teeth, that it is the most variable tooth in width (Table 3; Codrea et al. 2014: table 2).

(**6**) *A more complex cusp formula in P3*. The cusp formula of P3 is 2:5 in LPB (FGGUB) M.1700, compared to 2:3 in *B. transylvanicus* (Csiki-Sava et al. 2018). Again, we have no data on the variability of P3 in *B. transylvanicus* (Solomon et al. 2016: 327), including on the number of cusps. Nevertheless, in the kogaionid *H. belgica* the cusp formula of this position varies between 1:5 and 3:5 (Fig. 10u, v; De Bast and Smith 2017: fig. 5D, E). Krause (1977: 12) noted the high variability in the cusp number of P3 in ptilodontids, another family of multituberculates that also have unreduced P3, with four to seven cusps in *Ptilodus montanus* and four to six in *Ptilodus kummae*. The cusp formula also varies in *Prochetodon cavus*, which has a cusp formula of 4:4 or 5:4; this is observable on isolated teeth as well as specimens with associated teeth such as MCZ 20,039, a partial skull with P1-M2 on which P3 has a cusp formula of 4:4, and YPM-PU 14,034, a maxilla fragment with P1-3 on which P3 has a formula of 5:4 (Krause 1987).

(**7**) *Relatively more robust femur that is more lateromedially expanded at its distal end, with a wider intercondylar notch, and has a straight shaft*. Csiki-Sava et al. (2018) claimed that the femur known for LPB (FGGUB) M.1635 is slightly sigmoid by comparison with the one of LPB (FGGUB) M.1700. As explained here above (point 1), and as far as we know, this cannot be evaluated because the femur of LPB (FGGUB) M.1635 has not yet been described.

In addition to these seven features, which we interpret as variability or due to some damage and/or deformation of specimens, another important character that clearly unifies *B. transylvanicus* and *L. tholocephalos* is that they differ from all other kogaionids in the sub-rectangular shape of M1 with a short lingual row that bears only two clearly distinct cusps and a concave edge at the anterolingual part of the tooth. Therefore, based on our morphological analysis and the phylogenetic analysis, we here consider *Litovoi tholocephalos* as a junior synonym of *Barbatodon transylvanicus*.

Evolutionary Trends within Kogaionids and Plesiomophic Conditions within Cimolodontans

The new data provided by the small Maastrichtian *K. radulescui* and the integration of *B. oardaensis* and two Paleocene *Hainina* species in the updated multituberculate phylogeny allow better understanding of the position of kogaionids among cimolodontans.

Kogaionidae, already obtained in previous analyses as a polytomy (Smith and Codrea 2015) or with *K. ungureanui* as the basal taxon (Csiki-Sava et al. 2018; Wang et al. 2019; Weaver et al. 2020), is here confirmed as a monophyletic clade based on the analysis of seven kogaionid taxa. The addition of *K. radulescui*, *B. oardaensis*, and the *Hainina* species to the phylogenetic analysis elucidates an evolutionary trend within the clade (Fig. 11). The most plesiomorphic and oldest kogaionids *K. ungureanui*, *B. transylvanicus*, and *B. oardaensis* are in basal positions whereas the most complex and youngest *Hainina* species occur in apical positions in the kogaionid trees. Between the two, *K. radulescui* possesses one derived character by comparison with *B. oardaensis*. While *K. radulescui* is the most derived of the four Maastrichtian species in the trees, it is morphologically the most similar to *K. ungureanui*. However, as currently resolved, the phylogeny suggests that neither *Kogaionon* nor *Barbatodon* are monophyletic. Although the characters matrix has been much improved, this contrast suggests that it is not accurate enough to reflect entirely the morphological results. Several characters allowing to discriminate *Kogaionon* from *Barbatodon* are not taken into account in multituberculate phylogenies. Therefore, a better characterization of the character states, especially for P3 and P4, such as it has been done recently for the Djadochtatherioidea and some cimolodontans (Rougier et al. 2016; Wible et al. 2019) would probably be necessary to better discriminate phylogenetically the kogaionids.

In the evolutionary trends of kogaionids, we see the following as derived features: a decrease of P3 size, a labiolingually shortening of the anterior part of P4, a crestiform development of the last three cusps of the middle row of P4, an extension of the M1 lingual row in anterior direction, and an increase of cusp number in the M1 lingual row. If this pattern is confirmed, *Barbatodon* would represent the most plesiomorphic state and *Hainina* the most derived; *Kogaionon* would be morphologically intermediate.

The recognition of *Hainina* as a kogaionid (Peláez-Campomanes et al. 2000) and the improvement of the morphological knowledge of *Barbatodon* (Csiki et al. 2005; Codrea et al. 2014, 2017a; Smith and Codrea 2015; Solomon et al. 2016, 2021) allowed us to progressively characterize the endemic family Kogaionidae. The morphology of the latter is particularly plesiomorphic by comparison with most contemporaneous multituberculate groups, which have more complex teeth with higher numbers of cusps (Kielan-Jaworowska et al. 2004). Despite their Maastrichtian-Paleocene age, kogaionids indeed retain simple upper premolars, only four cusps in the middle (main) row of P4, only four cusps in the middle (main) row of M1, only two rows of three cusps on m1 (plus sometimes one extra labial cusp), and high ratios of upper premolar/molar length. These plesiomorphic features are present in numerous derived plagiaulacidans such as the Early Cretaceous plagiaulacids *Bolodon*, the eobaatarids *Eobaatar* and *Sinobaatar*, and the arginbaatarid *Arginbaatar* (Kielan-Jaworowska et al. 1987; Kusuhashi et al. 2009). The main difference in the upper dentition is the presence of only two incisors (I2 and I3), no canine and four upper premolars in kogaionids whereas several plagiaulacidans retain I1, a canine, and most of them have five premolars. So, even if kogaionids possess numerous plesiomorphic characters, their cimolodontan status appears indisputable. Due to this poorly understood cimolodontan dentition, kogaionids, based on *Kogaionon* and *Hainina*, were regarded as a separate family that could not be placed among established multituberculate superfamilies and therefore were assigned to a superfamily incertae sedis (Kielan-Jaworowska and Hurum 2001). *Barbatodon* was still, until recently, tentatively assigned to the basal cimolodontan *Paracimexomys* group (Kielan-Jaworowska et al. 2004).

The discovery of a partial cranium associated with lower jaws of *Barbatodon* allowed us to show that this kogaionid presents in fact a mosaic of primitive and derived characters, and that it is phylogenetically basal among Cimolodonta (Smith and Codrea 2015). These results are here confirmed. The most derived characters of kogaionids are probably the absence of p3 and the presence of a lingual cusp row on M1. These characters seem to follow the general tendency of most cimolodontan groups. However, other characters typical of kogaionids might be reinterpreted in light of recent progress made on allotherians. A first case is the large p4. It has been considered as a derived condition such as in ptilodontoids (Kielan-Jaworowska and Hurum 2001). Recently, Weaver and Wilson (2020) hypothesized that cimolodontans evolved a wide range of p4 shapes already by the mid-Cretaceous, and that p4 shape disparity remained stable through the Late Cretaceous. Our present work highlights the very large p4 in kogaionids (e.g., *B. transylvanicus*). It is noteworthy that Early Cretaceous eobaatarids also have a large p4, confirming that a large p4 is not inherently a derived condition. *Sinobaatar fuxinensis* from the Aptian-Albian Fuxin and Shahai formations in Liaoning, northeastern China has an especially large p4 by comparison with m1 (Kusuhashi et al. 2009), a difference in size that is comparable to what is seen in kogaionids. The width of the posterior part of p4 in *S. fuxinensis* and

Heishanobaatar triangulus from the Aptian-Albian Shahai and Fuxin formations in Liaoning is also similar to that of Maastrichtian kogaionids (Kusuhashi et al. 2009, 2010). Another even better example is *Liaobaatar* from the Aptian-Albian Fuxin Formation in Liaoning, which has an enormous p4 by comparison with p3 and m1 (Kusuhashi et al. 2009, 2020). Moreover, the latter has two rows of three cusps on m1 as in kogaionids. A second case of typical kogaionid character that might have misinterpreted is the diastema between I2 and I3, which is shorter than in most other groups of multituberculates. Because the four kogaionid skulls available have such a similar diastema present in small as well as large skulls we hypothesize that this short diastema is a feature shared by all kogaionids and may even be a symplesiomorphy shared with some eobaatarids. *Sinobaatar xiei* from the Aptian-Albian Fuxin Formation indeed has a diastema between I2 and I3 that is similar in length to the diastema between I3 and the posterior border of the premaxilla (Kusuhashi et al. 2009: fig. 5). This condition is similar to that of kogaionids. Therefore, we hypothesize that the position of I3 along the margin of the premaxilla at mid-distance of premaxillary length is probably the primitive condition in cimolodontans. This condition is also present in basal taeniolabidoids such as *Catopsalis alexanderi* from the early Danian Denver Formation, Colorado (Middleton 1982). It resembles the condition in ptilodontoids but the latter have a shorter premaxilla with I3 located on the posterior edge of the premaxilla. At the opposite, djadochtatherioids and eucosmodontids have a longer premaxilla with I3 more internally situated on the palate (Kielan-Jaworowska et al. 2004).

Origin of Kogaionids and Isolation of Europe

The origin of kogaionids is unknown but they are restricted to Europe and therefore considered to be endemic. They are also the only multituberculate family known from the Late Cretaceous of Europe and were restricted at that time to Eastern Europe. They are generally considered to be geographically isolated, as are several other European groups of vertebrates of the Late Cretaceous European archipelago (Csiki-Sava et al. 2015). Among the latter are numerous other Maastrichtian vertebrates from Transylvania retaining plesiomorphic characters: several alytid and bombinatorid anurans (Venczel et al. 2016), the paramacellodid *Becklesius*, teiid *Bicuspidon*, and barbatteiid lizards (Folie and Codrea 2005; Venczel and Codrea 2016; Codrea et al. 2017b), the turtle *Kallokibotion* (PerézGarcía and Codrea 2018; Martín-Jiménez et al. 2021), the crocodyliform *Allodaposuchus* (Delfino et al., 2008; Narváez et al. 2020), the atoposaurid crocodyliforms *Sabresuchus* and *Aprosuchus* (Martin et al. 2010; Tennant et al. 2016; Venczel and Codrea 2019), the iguanodontian *Zalmoxes* (Weishampel et al. 2003; Godefroit et al. 2009), the titanosaurians *Magyarosaurus* and *Paludititan* (Csiki et al. 2010), and the ankylosaurian *Struthiosaurus* (Kirkland et al. 2013). Csiki-Sava et al. (2015: 96) suggested that "these ancient lineages were sheltered in refugia all across Late Cretaceous Europe, a pattern that is again concordant with an insular, archipelago-type setting." The particular fauna of the Haţeg Basin led Nopcsa (1914) to propose the hypothesis of a long-lived, geographically isolated "Haţeg Island." The geographical surface of the island has been extended by several authors and the hypothesis has been reiterated many times, especially since the "Dinosaur Island" synthesis of Csiki and Grigorescu (2007) but is now debated (Krause et al. 2020: suppl. p. 26–38). In this framework, *Barbatodon* (= *Litovoi*) did not escape the rule and was also suspected as having unique adaptations, including iron pigmented dental enamel and a very small brain that evolved as a resident of "Haţeg Island" (Smith and Codrea 2015; Csiki-Sava et al. 2018). However, the features allowing to characterize an island, which are low species richness, taxonomic balance, high endemism, or relative "primitiveness," are perhaps not all present in the "Haţeg Island" (Krause et al. 2020). The primitiveness of kogaionid mammals, as is also the case for several other vertebrates on the so-called island, might be explained by the general isolation of Europe and not necessarily by insular conditions. The discovery of *K. radulescui*, a kogaionid smaller than *K. ungureanui* and *B. transylvanicus* but larger than *B. oardaensis* confirms a higher diversity of the family than previously thought (Table 3; Solomon et al. 2021). The presence of small-, middle-, and large-sized kogaionids is indeed not very supportive of insular conditions. The small size of several dinosaurs was already explained by the retention of primitive features instead of dwarfing in the case of nodosaurid ankylosaurs (Pereda-Suberbiola and Galton 2009) and the iguanodontian *Zalmoxes* (Ősi et al. 2012). The recent discovery of a gargantuavid theropod in Romania, a group supposed to have lost their flight capabilities in an insular environment of the Ibero-Armorican Island, challenges the hypothesis that this unusual taxon evolved under insular conditions and suggests that it belongs to a distinctive theropod clade of the Late Cretaceous European archipelago (Mayr et al. 2020). These arguments conflicting with the concept of "Haţeg Island" are rather in favor of a long isolation of a part of Europe during the Late Cretaceous. This supports estimated ghost lineages of 30 to 70 Myr among "Haţeg Island" vertebrates, varying for each group, with an estimation of 45–50 Myr for kogaionids (Weishampel et al. 2010).

If this hypothesis is correct, kogaionids would have been isolated for a long time in Europe, with several

plesiomorphic characters inherited from Early Cretaceous multituberculates being retained. Kogaionids have a conservative dental morphology, particularly striking when compared with that of djadochtatherioids and taeniolabidoids, which have several derived morphologies including even strong reduction or disappearance of upper premolar positions and increase in size or number of cusps of M1. Kogaionids retain four large upper premolars and limited cusp number on M1. M1 labial and lingual rows are variable in aspect and number of cusps in the different kogaionid species, however, the M1 middle row is stable with four cusps in all species. Among cimolodontans, only some taxa in the *Paracimexomys* group have a sufficiently plesiomorphic morphology to contend as potential ancestors of kogaionids (Kielan-Jaworowska et al. 2004). The Albian-Cenomanian *Bryceomys* indeed presents M1 with four cusps in the middle row and the beginning of a third lingual row with 2–3 cusps, and m2 with a cusp formula 3:2, as in kogaionids (Eaton and Cifelli 2001). However, P4 has five cusps on the main row and the m1 cusp formula is 4:3, which is more than the number of cusps on the same tooth positions in the most basal kogaionids (P4 with four cusps and some m1s with 3:3). So, even the oldest known cimolodontans, *Paracimexomys* and *Dakotamys* from the Cenomanian Dakota Formation of Utah, and *Cedaromys* and *Bryceomys* from the Albian-Cenomanian Cedar Mountain Formation of Utah (Eaton and Cifelli 2001), all belonging to the North American *Paracimexomys* group (Kielan-Jaworowska and Hurum 2001), might already be too derived to have given rise to kogaionids. Nevertheless, both groups are morphologically close. In Asia, *Sinobaatar* and other Early Cretaceous eobaatarid multituberculates from China seem to be better potential ancestors of kogaionids. These Asian multituberculates share with kogaionids the following features: limited cusp numbers, diastema between I2 and I3, presence of large upper premolars, P1 with three cusps, P2 with four cusps and a posterior flat extension, four cusps on the last upper premolar labial row (but six in *Hakusanobaatar*; Kusuhashi 2008), four cusps on M1 middle row, long and high p4 with a limited number of serrations and ridges, and high ratio of P1-P4(P5)/M1-2 length (Kielan-Jaworowska et al. 1987; Kusuhashi et al. 2009, 2010). These potential ancestors of the earliest cimolodontans could have dispersed from Asia during the early Late Cretaceous or more possibly be already present in the Early Cretaceous of Europe (Sweetman 2009; Badiola et al. 2011; Martin et al. 2021). This eobaatarid hypothesis is supported by their high diversity and dental plasticity, some taxa such as *Dolichoprion* from the Aptian-Albian Fuxin Formation of China having a p2 reduced or absent (Kusuhashi et al. 2020). Others such as *Eobaatar clemensi* from the Barremian Wessex Formation of England have m1 with a labial cingulum that surrounds the third posterolabial cusp, similar to the condition in kogaionids (Sweetman 2009).

In conclusion, our study suggests that kogaionids originated from an eobaatarid-like ancestor dispersing from Asia or possibly already existing in Europe between the Barremian and Albian. Due to their Maastrichtian-Paleocene age, kogaionids have to originate from older and more basal cimolodontans retaining p3, and which were probably morphologically close to some early members of the informative *Paracimexomys* group. The latter needs a thorough revision, as it has been started (Weaver et al. 2020), in order to better characterize the Albian-Cenomanian early members (e.g., *Bryceomys*, *Cedaromys*) and confirm their cimolodontan status on the basis of the recent progress in multituberculate phylogeny.

Supplementary Information The online version contains supplementary material available at https://doi.org/10.1007/s10914-021-09564-7.

Acknowledgements We thank all members of our field team who participated in the paleontological expeditions in Transylvania since 2000. At RBINS we thank Julien Cillis, Eric De Bast, and Nathan Vallée-Gillette for assistance with SEM and optical photographs, Nathalie Van Hoey for preparation and casting, and Annelise Folie for table and electronic supplementary material formatting. We thank Zoltán Csiki-Sava (University of Bucharest) for photographs of *Kogaionon ungureanui*. We are grateful to reviewers Nao Kusuashi (Ehime University) and David W. Krause (Denver Museum of Nature & Science) and editor John Wible for thorough comments that led to significant improvements in the manuscript. This work was supported by the Belgian Science Policy Office project MO/36/001-004 (to TS), a grant from the Ministry of Research, Innovation and Digitization, CNCS/CCCDI – UEFISCDI, project number PD136/2020, within PNCDI III (to AAS), and Babeș-Bolyai University grants AGC 30362, 34783, 34782 (to VAC).

References

Archibald JD (1982) A study of Mammalia and geology across the Cretaceous–Tertiary boundary in Garfield County, Montana. Univ Calif Publ Geol Sci 122:1–286

Averianov AO, Martin T, Lopatin AV, Schultz JA, Schellhorn R, Krasnolutskii S, Skutschas P, Ivantsov S (2020) Multituberculate mammals from the Middle Jurassic of western Siberia, Russia, and the origin of Multituberculata. Pap Palaeontol 7:769–787. https://doi.org/10.1002/spp2.1317

Badiola A, Canudo JI, Cuenca-Bescós G (2011) A systematic reassessment of Early Cretaceous multituberculates from Galve (Teruel, Spain). Cretac Res 32:45–57. https://doi.org/10.1016/j.cretres.2010.10.003

Codrea V, Dica P (2005) Upper Cretaceous-lowermost Miocene lithostratigraphic units exposed in Alba Iulia-Sebeș-Vinţu de Jos area (SW Transylvanian Basin). Stud Univ Babes-Bolyai Geol 50: 19–26

Codrea V, Smith T, Dica P, Folie A, Garcia G, Godefroit P, Van Itterbeeck J (2002) Dinosaur egg nests, mammals and other vertebrates from a new Maastrichtian site of the Haţeg Basin (Romania). C R Palevol 1:173–180. https://doi.org/10.1016/S1631-0683(02)00021-0

Codrea V, Solomon A, Venczel M, Smith T (2014) A new kogaionid multituberculate mammal from the Maastrichtian of the

Transylvanian Basin, Romania. C R Palevol 13:489–499. https://doi.org/10.1016/j.crpv.2016.04.002
Codrea V, Solomon A, Venczel M, Smith T (2017a) First mammal species identified from the Upper Cretaceous of the Rusca Montană Basin (Transylvania, Romania). C R Palevol 16:27–38. https://doi.org/10.1016/j.crpv.2016.04.002
Codrea VA, Venczel M, Solomon A (2017b) A new family of teiioid lizards from the Upper Cretaceous of Romania with notes on the evolutionary history of early teiioids. Zool J Linnean Soc 181:385–399. https://doi.org/10.1093/zoolinnean/zlx008
Codrea V, Vremir M, Jipa C, Godefroit P, Csiki Z, Smith T, Fărcaş C (2010) More than just Nopcsa's Transylvanian dinosaurs: a look outside the Haţeg Basin. Palaeogeogr Palaeoclimatol Palaeoecol 293:391–405. https://doi.org/10.1016/j.palaeo.2009.10.027
Cope ED (1884) The Tertiary Marsupialia. Am Nat 18:686–697. https://doi.org/10.1086/273711
Csiki Z, Codrea V, Jipa-Murzea C, Godefroit P (2010) A partial titanosaur (Sauropoda, Dinosauria) skeleton from the Maastrichtian of Nălaţ-Vad, Haţeg Basin, Romania. N Jb Geol Paläontol Abh 258:297–324. https://doi.org/10.1127/0077-7749/2010/0098
Csiki Z, Grigorescu D (2000) Teeth of multituberculate mammals from the Late Cretaceous of Romania. Acta Palaeontol Pol 45:85–90
Csiki Z, Grigorescu D (2007) The "Dinosaur Island" - new interpretation of the Haţeg vertebrate fauna after 110 years. Sargetia 20:5–26
Csiki Z, Grigorescu D, Rücklin M (2005) A new multituberculate specimen from the Maastrichtian of Pui, Romania and reassessment of affinities of *Barbatodon*. Acta Palaeontol Rom 5:73–86
Csiki-Sava Z, Buffetaut E, Ősi A, Pereda-Suberbiola X, Brusatte SL (2015) Island life in the Cretaceous faunal composition, biogeography, evolution, and extinction of land-living vertebrates on the Late Cretaceous European archipelago. ZooKeys 469:1–161. https://doi.org/10.3897/zookeys.469.8439
Csiki-Sava Z, Vremir M, Vasile Ş, Brusatte SL, Dyke G, Naish D, Norell M, Totoianu R (2016) The East Side Story – The Transylvanian latest Cretaceous continental vertebrate record and its implications for understanding Cretaceous-Paleogene boundary events. Cretac Res 57:662–698. https://doi.org/10.1016/j.cretres.2015.09.003
Csiki-Sava Z, Vremir M, Meng J, Brusatte SL, Norell MA (2018) Dome-headed, small-brained island mammal from the Late Cretaceous of Romania. Proc Natl Acad Sci USA 115:4857–4862. https://doi.org/10.1073/pnas.1801143115
De Bast E, Smith T (2017) The oldest Cenozoic mammal fauna of Europe: implication of the Hainin reference fauna for mammalian evolution and dispersals during the Paleocene. J Syst Palaeontol 15:741–785. https://doi.org/10.1080/14772019.2016.1237582
Delfino M, Codrea V, Folie A, Dica P, Godefroit P, Smith T (2008) A complete skull of *Allodaposuchus precedens* Nopcsa, 1928 (Eusuchia) and a reassessement of the morphology of the taxon based on the Romanian remains. J Vertebr Paleontol 28: 111–122. https://doi.org/10.1671/0272-4634(2008)28[111:ACSOAP]2.0.CO;2
Eaton JG (1995) Cenomanian and Turonian (early Late Cretaceous) multituberculate mammals from southwestern Utah. J Vertebr Paleontol 15:761–784
Eaton JG, Cifelli RL (2001) Multituberculate mammals from near the Early–Late Cretaceous boundary, Cedar Mountain Formation, Utah. Acta Palaeontol Pol 46:453–518
Folie A, Codrea V (2005) New lissamphibians and squamates from the Maastrichtian of Haţeg Basin, Romania. Acta Palaeontol Pol 50:57–71
Fosse G, Rădulescu C, Samson P-M (2001) Enamel microstructure of the Late Cretaceous multituberculate mammal *Kogaionon*. Acta Palaeontol Pol 46:437–440
Fox RC (2005) Microcosmodontid multituberculates (Allotheria, Mammalia) from the Paleocene and Late Cretaceous of western Canada. Palaeontolographica Canadiana 23:1–109
Gheerbrant E, Codrea V, Hosu Al, Sen S, Guernet C, de Lapparent de Broin F, Riveline J (1999) Découverte de vertébrés dans les Calcaires de Rona (Thanétien ou Sparnacien), Transylvanie, Roumanie: les plus anciens mammifères cénozoïques d'Europe orientale. Eclogae Geol Helv 92:517–535
Godefroit P, Codrea V, Weishampel DB (2009) Osteology of *Zalmoxes shqiperorum* (Dinosauria, Ornithopoda), based on new specimens from the Upper Cretaceous of Nălaţ-Vad (Romania). Geodiversitas 31:525–553. https://doi.org/10.5252/g2009n3a3
Grigorescu D, Hahn G (1987) The first multituberculate teeth from the Upper Cretaceous of Europe (Romania). Geol et Palaeontol 21:237–243
Grigorescu D, Venczel M, Csiki Z, Limberea R (1999) New latest Cretaceous microvertebrate fossil assemblages from the Haţeg Basin (Roumania). Geol en Mijnb 78:301–314
Hurum JH (1998) The inner ear of two Late Cretaceous multituberculate mammals, and its implications for multituberculate hearing. J Mammal Evol 5:65–93
Jepsen GL (1940) Paleocene faunas of the Polecat Bench Formation, Park County, Wyoming: Part I. Proc Am Philos Soc 83:217–341
Kielan-Jaworowska Z, Cifelli RL, Luo Z-X (2004) Mammals from the Age of Dinosaurs: Origins, Evolution and Structure. Columbia University Press, New York
Kielan-Jaworowska Z, Dashzeveg D, Trofimov BA (1987) Early Cretaceous multituberculates from Mongolia and a comparison with Late Jurassic forms. Acta Palaeontol Pol 32:3–47
Kielan-Jaworowska Z, Gambaryan P (1994) Postcranial anatomy and habits of Asian multituberculate mammals. Foss and Strat 36:1–92
Kielan-Jaworowska Z, Hurum JH (1997) Djadochtatheria – a new suborder of multituberculate mammals. Acta Palaeontol Pol 42:201-242
Kielan-Jaworowska Z, Hurum JH (2001) Phylogeny and systematics of multituberculate mammals. Palaeontology 44:389–429. https://doi.org/10.1111/1475-4983.00185
Kielan-Jaworowska Z, Hurum JH, Badamgarav D (2003) An extended range of multituberculate *Kryptobaatar* and distribution of mammals in the Upper Cretaceous of the Gobi Desert. Acta Palaeontol Pol 48:273–278
Kielan-Jaworowska Z, Lancaster TE (2004) A new reconstruction of multituberculate endocranial casts and encephalization quotient of *Kryptobaatar*. Acta Palaeontol Pol 49:177–188
Kielan-Jaworowska Z, Sochava AV (1969) The first multituberculate from the uppermost Cretaceous of the Gobi Desert (Mongolia). Acta Palaeontol Pol 14:355–367
Kirkland JI, Alcalá L, Loewen MA, Espílez E, Mampel L, Wiersma JP (2013) The basal nodosaurid ankylosaur *Europelta carbonensis* n. gen., n. sp. from the Lower Cretaceous (Lower Albian) Escucha Formation of northeastern Spain. PLoS ONE 8(12):e80405. https://doi.org/10.1371/journal.pone.0080405
Krause DW (1977) Paleocene multituberculates (Mammalia) of the Roche Percée local fauna, Ravenscrag Formation, Saskatchewan, Canada. Palaeontographica Abt A 159:1–36
Krause DW (1980) Multituberculates from the Clarkforkian Land-Mammal Age, late Paleocene-early Eocene, of western North America. J Paleontol 54:1163–1183
Krause DW (1982a) Multituberculates from the Wasatchian Land-Mammal Age, early Eocene, of western North America. J Paleontol 56:271–294
Krause DW (1982b) Jaw movement, dental function, and diet in the Paleocene multituberculate *Ptilodus*. Paleobiology 8:265–281
Krause DW (1987) Systematic revision of the genus *Prochetodon* (Ptilodontidae, Multituberculata) from the late Paleocene and early Eocene of western North America. Contrib Mus Paleontol, Univ Michigan 27:221–236

Krause DW, Hoffmann S, Hu Y, Wible JR, Rougier GW, Kirk EC, Groenke JR, Rogers RR, Rossie JB, Schultz JA, Evans AR, von Koenigwald W, Rahantarisoa LJ (2020) Skeleton of a Cretaceous mammal from Madagascar reflects long-term insularity. Nature 581:421–427. https://doi.org/10.1038/s41586-020-2234-8

Kusuhashi N (2008) Early Cretaceous multituberculate mammals from the Kuwajima Formation (Tetori Group), central Japan. Acta Palaeontol Pol 53:379–390

Kusuhashi N, Hu Y-M, Wang Y-Q, Setoguchi T, Matsuoka H (2009) Two eobaatarid (Multituberculata; Mammalia) genera from the Lower Cretaceous Shahai and Fuxin formations, northeastern China. J Vertebr Paleontol 29:1264–1288

Kusuhashi N, Hu Y, Wang Y, Setogushi T, Matsuoka H (2010) New multituberculate mammals from the Lower Cretaceous (Shahai and Fuxin formations), northeastern China. J Vertebr Paleontol 30:1501–1514

Kusuhashi N, Wang Y-Q, Jin X (2020) A new eobaatarid multituberculate (Mammalia) from the Lower Cretaceous Fuxin Formation, Fuxin-Jinzhou Basin, Liaoning, northeastern China. J Mammal Evol 27:605–623. https://doi.org/10.1007/s10914-019-09481-w

Linnaeus C (1758) Systema naturae per regna tria naturae, secundum classes, ordines, genera, species, cum characteribus, differentiis, synonymis, locis.Vol. 1: Regnum animale. Editio decimal reformata. Laurentii Salvii, Stockholm

Mao FY, Liu C, Chase MH, Smith AK, Meng J (2020) Exploring ancestral phenotypes and evolutionary development of the mammalian middle ear based on Early Cretaceous Jehol mammals. Natl Sci Rev nwaa188. https://doi.org/10.1093/nsr/nwaa188

Mao F-Y, Wang Y-Q, Meng J (2016) New specimens of the multituberculate mammalian *Sphenopsalis* from the Paleocene of Inner Mongolia, China: implications for phylogeny and biology of taeniolabidoid multituberculates. Acta Palaeontol Pol 61:429–454. https://doi.org/10.4202/app.00117.2014

Marsh OC (1880) Notice on Jurassic mammals representing two new orders. Am J Sci 20:235–239. https://doi.org/10.2475/ajs.s3-20.117.235

Martin JE, Rabi R, Csiki Z (2010) Survival of *Theriosuchus* (Mesoeucrocodylia: Atoposauridae) in a Late Cretaceous archipelago: a new species from the Maastrichtian of Romania. Naturwissenschaften 9:845–854. https://doi.org/10.1007/s00114-010-0702-y

Martin T, Averianov AO, Schultz JA, Schwermann AH (2021) First multituberculate mammals from the Early Cretaceous of Germany. Cretac Res 119:104699. https://doi.org/10.1016/j.cretres.2020.104699

Martin-Jiménez M, Codrea V, Pérez-García A (2021) Neuroanatomy of the European uppermost Cretaceous stem turtle *Kallokibotion bajazidi*. Cretac Res 120:104720. https://doi.org/10.1016/j.cretres.2020.104720

Mayr G, Codrea V, Solomon A, Bordeianu M, Smith T (2020) A well-preserved pelvis from the Maastrichtian of Romania suggests that the enigmatic *Gargantuavis* is neither an ornithurine bird nor an insular endemic. Cretac Res 106:104271. https://doi.org/10.1016/j.cretres.2019.104271

McKenna MC (1975) Toward a phylogenetic classification of the Mammalia. In: Luckett WP, Szalay FS (eds) Phylogeny of the Primates. Plenum Press, New York, pp 21–46. https://link.springer.com/chapter/. https://doi.org/10.1007/978-1-4684-2166-8_2

Middleton MD (1982) A new species and additional material of *Catopsalis* (Mammalia, Multituberculata) from the Western Interior of North America. J Paleontol 56:1197–1206. https://www.jstor.org/stable/1304576

Narváez I, Brochu AC, De Celis A, Codrea V, Escaso F, Pérez-García A, Ortega F (2020) New diagnosis for *Allodaposuchus precedens*, the type species of the European Upper Cretaceous clade Allodaposuchidae. Zool J Linnean Soc 189:618–634. https://doi.org/10.1093/zoolinnean/zlz029

Nopcsa F (1914) Über das Vorkommen der Dinosaurier in Siebenbürgen. Verh zool-bot Ges Wien 54:12–14

Ősi A, Prondvai E, Butler R, Weishampel DB (2012) Phylogeny, histology and inferred body size evolution in a new rhabdodontid dinosaur from the Late Cretaceous of Hungary. PLoS One 7:e44318. https://doi.org/10.1371/journal.pone.0044318

Peláez-Campomanes P, López-Martinez N, Álvarez-Sierra MA, Daams R (2000) The earliest mammal of the European Paleocene: the multituberculate *Hainina*. J Paleontol 74:701–711. https://doi.org/10.1666/0022-3360(2000)074<0701:TEMOTE>2.0.CO;2

Pereda-Suberbiola X, Galton PM (2009) Dwarf dinosaurs in the latest Cretaceous of Europe? In: Colectivo Arqueológico-Paleontológico Salense (ed) IV Jornadas Internacionales sobre Paleontología de Dinosaurios y su Entorno. Actas, Salas de los Infantes, Burgos (Spain) 263–272

Peréz-García A, Codrea V (2018) New insights on the anatomy and systematics of *Kallokibotion* Nopcsa, 1923, the enigmatic uppermost Cretaceous basal turtle (stem Testudines) from Transylvania. Zool J Linnean Soc 182:419–443. https://doi.org/10.1093/zoolinnean/zlx037

Rădulescu C, Samson P (1986) Précisions sur les affinités des multituberculés (Mammalia) du Crétacé supérieur de Roumanie. C R Acad Sci 303:1825–1830

Rădulescu C, Samson P (1996) The first multituberculate skull from the Late Cretaceous (Maastrichtian) of Europe (Haţeg Basin, Romania). An Inst Geol Rom Abstracts 69:177–178

Rădulescu C, Samson P (1997) Late Cretaceous Multituberculata from the Haţeg Basin (Romania). Sargetia 17:247–255

Rigby JK Jr (1980) Swain quarry of the Fort Union Formation, middle Paleocene (Torrejonian), Carbon County, Wyoming: geologic setting and mammalian fauna. Evol Monogr 3:1-151

Rougier GW, Novacek MJ, Dashzeveg D (1997) A new multituberculate from the Late Cretaceous locality Ukhaa Tolgod, Mongolia. Considerations on multituberculate interrelationships. Am Mus Novitates 3191:1–26

Rougier GW, Sheth AS, Spurlin BK, Bolortsetseg M, Novacek MJ (2016) Craniodental anatomy of a new Late Cretaceous multituberculate mammal from Udan Sayr, Mongolia. Palaeontol Pol 67:197–248. https://doi.org/10.4202/pp.2016.67_197

Simpson GG (1937) Skull structure of the Multituberculata. Bull Am Mus Nat Hist 73:727–763

Sloan RE (1979) Multituberculata. In: Fairbridge RW, Jablonski D (ed) Paleontology. Encyclopedia of Earth Science. Springer, Berlin, Heidelberg, pp 492–498

Sloan RE, Van Valen L (1965) Cretaceous mammals from Montana. Science 148:220–227

Smith T, Codrea V (2015) Red iron-pigmented tooth enamel in a multituberculate mammal from the Late Cretaceous Transylvanian "Haţeg Island." PLoS One 10:e0132550. https://doi.org/10.1371/journal.pone.0132550

Smith T, Codrea V, Sasaran E, Van Itterbeeck J, Bultynck P, Csiki Z, Dica P, Fărcaș C, Folie A, Garcia G, Godefroit P (2002) A new exceptional vertebrate site from the Late Cretaceous of the Haţeg Basin (Romania). Stud Univ Babes-Bolyai Geol Spec issue 1:321–330

Solomon A, Codrea V, Venczel M, Dumbravă M, Smith T (2016) New remains of the multituberculate mammal *Barbatodon* from the Upper Cretaceous of the Haţeg Basin (Romania). J Mammal Evol 23:319–335. https://doi.org/10.1007/s10914-016-9322-4

Solomon AA, Codrea VA, Venczel M, Grellet-Tinner G (2020) A new species of large-sized pterosaur from the Maastrichtian of Transylvania (Romania). Cretac Res 110:104316. https://doi.org/10.1016/j.cretres.2019.104316

Solomon A, Codrea V, Venczel M, Smith T (2021) New data on *Barbatodon oardaensis*, the smallest Late Cretaceous multituberculate mammal from Europe. C R Palevol, in press

Sweetman SC (2009) A new species of the plagiaulacoid multituberculate mammal *Eobaatar* from the Early Cretaceous of southern Britain. Acta Palaeontol Pol 54:373–384. https://doi.org/10.4202/app.2008.0003

Swofford DL (2003) PAUP*. Phylogenetic analysis using parsimony (*and other methods). Version 4. Sinauer Associates, Sunderland, MA

Tennant JP, Mannion PD, Upchurch P (2016) Evolutionary relationships and systematics of Atoposauridae (Crocodylomorpha: Neosuchia): implications for the rise of Eusuchia. Zool J Linnean Soc 177:854–936. https://doi.org/10.1111/zoj.12400

Van Itterbeeck J, Markevich V, Codrea V (2005) Palynostratigraphy of the Maastrichtian dinosaur and mammal sites of the Râul Mare and Barbat valleys (Haţeg Basin, Romania). Geol Carp 56:137–147

Van Itterbeeck J, Săsăran E, Codrea V, Săsăran L, Bultynck P (2004) Sedimentology of the Upper Cretaceous mammal- and dinosaur-bearing sites along the Râul Mare and Bărbat rivers, Haţeg Basin, Romania. Cretac Res 25:517–530. https://doi.org/10.1016/j.cretres.2004.04.004

Venczel M, Codrea VA (2016) A new teiid lizard from the Late Cretaceous of the Haţeg Basin, Romania and its phylogenetic and palaeobiogeographical relationships. J Syst Palaeontol 14:219–237. https://doi.org/10.1080/14772019.2015.1025869

Venczel M, Codrea VA (2019) A new *Theriosuchus*-like crocodyliform from the Maastrichtian of Romania. Cretac Res 100:24–38. https://doi.org/10.1016/j.cretres.2019.03.018

Venczel M, Gardner JD, Codrea VA, Csiki-Sava Z, Vasile Ş, Solomon AA (2016) New insights into Europe's most diverse Late Cretaceous anuran assemblage from the Maastrichtian of western Romania. Palaeobio Palaeoenv 96:61–95. https://doi.org/10.1007/s12549-015-0228-6

Vianey-Liaud M (1979) Les mammifères montiens de Hainin (Paléocène moyen de Belgique). Part I: Multituberculés. Palaeovertebrata 9:117–131

Vianey-Liaud M (1986) Les multitubercules thanétiens de France, et leurs rapports avec les multituberculés nord-américains. Palaeontographica A 191:85–171

Vremir M, Bălc R, Csiki-Sava Z, Brusatte SL, Dyke G, Naish D, Norell MA (2014) Petreşti-Arini – An important but ephemeral Upper Cretaceous continental vertebrate site in the southwestern Transylvanian Basin, Romania. Cretac Res 49:13–38. https://doi.org/10.1016/j.cretres.2014.02.002

Wang H, Meng J, Wang Y (2019) Cretaceous fossil reveals a new pattern in mammalian middle ear evolution. Nature 576:102–105. https://doi.org/10.1038/s41586-019-1792-0

Wang X, Dyke GJ, Codrea V, Godefroit P, Smith T (2011) A euenantiornithine bird from the Late Cretaceous Haţeg Basin of Romania. Acta Palaeontol Pol 56:853–857. https://doi.org/10.4202/app.2010.0085

Weaver LN, Wilson GP (2020) Shape disparity in the blade-like premolars of multituberculate mammals: functional constraints and the evolution of herbivory. J Mammal 102:967–985. https://doi.org/10.1093/jmammal/gyaa029

Weaver LN, Varricchio DJ, Sargis EJ, Chen M, Freimuth WJ, Wilson Mantilla GP (2020) Early mammalian social behaviour revealed by multituberculates from a dinosaur nesting site. Nat Ecol Evol 5:32–37. https://doi.org/10.1038/s41559-020-01325-8

Weishampel DB, Csiki Z, Benton MJ, Grigorescu D, Codrea V (2010) Palaeobiogeographic relationships of the Haţeg biota — between isolation and innovation. Palaeogeogr Palaeoclimatol Palaeoecol 293:419–437. https://doi.org/10.1016/j.palaeo.2010.03.024

Weishampel DB, Jianu CM, Csiki Z, Norman DB (2003) Osteology and phylogeny of *Zalmoxes* (n. g.), an unusual euornithopod dinosaur from the latest Cretaceous of Romania. J Syst Palaeontol 1: 65-123. https://doi.org/10.1017/S1477201903001032

Wible JR, Rougier GW (2000) Cranial anatomy of *Kryptobaatar dashzevegi* (Mammalia, Multituberculata), and its bearing on the evolution of mammalian characters. Bull Am Mus Nat Hist 247:1–124

Wible JR, Shelley SL, Bi S (2019) New genus and species of djadochtateriid multituberculate (Allotheria, Mammalia) from the Upper Cretaceous Bayan Mandahu Formation of Inner Mongolia. Ann Carnegie Mus 85:285–327. https://doi.org/10.2992/007.085.0401

Williamson TE, Brusatte SL, Secord R, Shelley SL (2016) A new taeniolabidoid multituberculate (Mammalia) from the middle Puercan of the Nacimiento Formation, New Mexico, and a revision of taeniolabidoid systematics and phylogeny. Zool J Linnean Soc 177:183–208. https://doi.org/10.1111/zoj.12336

Wilson GP, Evans AR, Corfe IJ, Smits PD, Fortelius M, Jernall J (2012) Adaptive radiation of multituberculate mammals before the extinction of dinosaurs. Nature 483:457–460. https://doi.org/10.1038/nature10880

Xu L, Zhang X, Pu H, Jia S, Zhang J, Lü J, Meng J (2015) Largest known Mesozoic multituberculate from Eurasia and implications for multituberculates evolution and biology. Sci Rep 5:14950. https://doi.org/10.1038/srep14950

Yuan C-X, Ji Q, Meng Q-J, Tabrum AR, Luo Z-X (2013) Earliest evolution of multituberculate mammals revealed by a new Jurassic fossil. Science 341:779–783. https://doi.org/10.1126/science.1237970